TURUN YLIOPISTON JULKAISUJA
ANNALES UNIVERSITATIS TURKUENSIS

SARJA - SER. A I OSA - TOM. 469

ASTRONOMICA - CHEMICA - PHYSICA - MATHEMATICA

MEMORY EFFECTS IN THE DYNAMICS OF OPEN QUANTUM SYSTEMS

by

Elsi-Mari Laine

TURUN YLIOPISTO
UNIVERSITY OF TURKU
Turku 2013

From

Department of Physics and Astronomy
University of Turku
Finland

Supervised by

Jyrki Piilo
Docent of Theoretical Physics
Department of Physics and Astronomy
University of Turku
Finland

Reviewed by

Barry Garraway
Reader in Theoretical Physics
Department of Physics and Astronomy
University of Sussex
UK

Jukka Pekola
Professor of Physics
Low Temperature Laboratory
Aalto University
Finland

Opponent

Matteo Paris
Professor of Physics
Department of Physics
Università degli Studi di Milano
Italy

ISBN 978-951-29-5496-4 (PRINT)
ISBN 978-951-29-5497-1 (PDF)
ISSN 0082-7002
Painosalama Oy - Turku, Finland 2013

Acknowledgments

Doing research is not a one-man job. Although this Thesis carries my name, it is the result of a contribution of many whom I wish to thank.

My foremost gratitude is towards my supervisor Jyrki. Thank you for sharing your scientific knowledge and professional experience with me. To become a good physicist one has to learn many things, also other than physics, and I have learned a great deal from you.

I also want to thank all the people I have had the chance to collaborate with: Heinz-Peter, Chuan-Feng, Biheng, Bassano, Andrea, Manuel and many others. Thank you for sharing your knowledge and ideas with me. It has been a pleasure working with you.

Not only will I remember these years for the physics but also for the wonderful outreach projects in which I had the chance to play a part. Thank you Sabrina for including me in all the exciting projects. The experiences I have gained from them are priceless.

I also want to thank Kalle-Antti and other people at the physics department for the great working atmosphere at the University of Turku. Surely, the one thing that has made these years so memorable is the people at the office. Both at the "corridor" in Turku and in the Edinburgh office. Thanks to all of you for being awesome. I especially want to thank Pinja for her friendship throughout the nine years of studies at the University of Turku.

I also wish to thank my family and friends for their endless support. It means the world to me. Finally, I want to thank Massimo for his love and backbone in rocky times. No words can rightly describe my gratitude. Thank you for existing.

Contents

Abstract

In this Thesis various aspects of memory effects in the dynamics of open quantum systems are studied. We develop a general theoretical framework for open quantum systems beyond the Markov approximation which allows us to investigate different sources of memory effects and to develop methods for harnessing them in order to realise controllable open quantum systems.

In the first part of the Thesis a characterisation of non-Markovian dynamics in terms of information flow is developed and applied to study different sources of memory effects. Namely, we study nonlocal memory effects which arise due to initial correlations between two local environments and further the memory effects induced by initial correlations between the open system and the environment.

The last part focuses on describing two all-optical experiment in which through selective preparation of the initial environment states the information flow between the system and the environment can be controlled. In the first experiment the system is driven from the Markovian to the non-Markovian regime and the degree of non-Markovianity is determined. In the second experiment we observe the nonlocal nature of the memory effects and provide a novel method to experimentally quantify frequency correlations in photonic environments via polarisation measurements.

List of articles

This thesis consists of an introductory review and the following six articles:

I H.-P. Breuer, E.-M. Laine, and J. Piilo,
Measure for the degree of non-Markovian behavior of quantum processes in open systems
Phys. Rev. Lett. **103**, 210401 (2009).

II E.-M. Laine, J. Piilo, and H.-P. Breuer
Measure for the Non-Markovianity of Quantum Processes
Phys. Rev. A **81**, 062115 (2010).

III E.-M. Laine, J. Piilo, and H.-P. Breuer
Witness for initial system-environment correlations in open system dynamics
EPL **92** 60010 (2010).

IV B.-H. Liu, L. Li, Y.-F. Huang, C.-F. Li, G.-C. Guo, E.-M. Laine, H.-P. Breuer, and J. Piilo
Experimental control of the transition from Markovian to non-Markovian dynamics of open quantum systems
Nature Physics **7**, 931-934 (2011).

V E.-M. Laine, H.-P. Breuer, J. Piilo, C.-F. Li, and G.-C. Guo
Nonlocal memory effects in the dynamics of open quantum systems
Phys. Rev. Lett. **108**, 210402 (2012).

VI B.-H. Liu, D.-Y. Cao, Y.-F. Huang, C.-F. Li, G.-C. Guo, E.-M. Laine, H.-. Breuer, and J. Piilo
Photonic realization of nonlocal memory effects and non-Markovian quantum probes
Scientific Reports **3**, 1781 (2013).

Other published material

This is a list of the publications produced which have not been chosen as a part of the doctoral thesis:

I E.-M. Laine
A quantum jump description for the non-Markovian dynamics of the spin-boson model
Phys. Scr. T **140**, 014053 (2010).

II L. Mazzola, E.-M. Laine, H.-P. Breuer, S. Maniscalco, and J. Piilo
Phenomenological memory-kernel master equations and time-dependent Markovian processes
Phys. Rev. A **81**, 062120 (2010).

III B. Vacchini, A. Smirne, E.-M. Laine, J. Piilo, and H.-P. Breuer
Markovian and non-Markovian dynamics in quantum and classical systems
New J. Phys. **13**, 093004 (2011).

IV J.-S. Tang, C.-F. Li, Y.-L. Li, X.-B. Zou, G.-C. Guo, H.-P. Breuer, E.-M. Laine, and J. Piilo
Measuring non-Markovianity of processes with controllable system-environment interaction
EPL **97**, 10002 (2012).

V M. Gessner, E.-M. Laine, H.-P. Breuer, and J. Piilo
Correlations in quantum states and the local creation of quantum discord
Phys. Rev. A **85**, 052122 (2012).

VI E.-M. Laine, K. Luoma, and J. Piilo
Local in time master equations with memory effects: Applicability and interpretation
J. Phys. B: At. Mol. Opt. Phys. **45**, 154004 (2012).

VII A. Smirne, E.-M. Laine, H.-P. Breuer, J. Piilo, and B. Vacchini
Role of correlations in the thermalization of quantum systems
New J. Phys. **14**, 113034 (2012).

VIII S. Wissmann, A. Karlsson, E.-M. Laine, J. Piilo, and H.-P. Breuer
Optimal state pairs for non-Markovian quantum dynamics
Phys. Rev. A **86**, 062108 (2012).

Chapter 1

Introduction

In quantum theory the time evolution of a system is given by a deterministic wave equation, the Schrödinger equation. Yet, observed quantum objects often exhibit irreversible behaviour not predicted by the standard theory. Irreversibility in the dynamics arises when the quantum system interacts with the external world or when the deterministic evolution of the system is interrupted by a measurement process. A quantum system, which is influenced by the interaction with its surroundings is called an open quantum system.

Nearly all realistic quantum systems are open, and thus understanding and controlling of the dynamics rising from the presence of the environment is of central importance in present research. Indeed, open quantum systems have been studied in a variety of physical systems ranging from quantum optical to solid state or chemical systems. The methods traditionally used by the different communities vary greatly, and therefore, the development of an universal theory of open quantum systems is challenging.

The initial attempts to tackle open quantum systems were concentrating on microscopic modelling via Markovian master equations [1, 2]. The first general description involved the theory of dynamical semigroups giving rise to stationary and memoryless Markovian dynamics [3–5]. The Markovian description is sufficient for a wide class of open systems, but it fails in the presence of strong system-environment couplings and structured or finite reservoirs. As these properties are encountered in quantum mechanics experiments to an increasing extent, efficient methods for treating non-Markovian dynamics are needed. Thus, non-Markovian open quantum systems have been extensively studied in the last decades and various analytical methods and numerical simulation techniques have been developed in order to give insights into the nature of non-Markovian effects [6–8].

The aim of this Thesis is to develop a general theoretical framework for open quantum systems beyond the Markov approximation and to give insights into various features of memory effects. The objective is, in particular, to shed light on the different sources of memory effects and to further develop methods for harnessing them in order to realise controllable open quantum systems that could be used for e.g. probing some specific environment properties [9–13] or as a resource for quantum technologies [14–16].

Apart from the methodology, a lot of attention has been recently focused on fundamental aspects of non-Markovian quantum dynamics, since no general consistent theory has been available. Indeed, even a clearcut definition of Markovian dynamics in the quantum realm has for long been missing. In the research articles I and II a characterisation of non-Markovian dynamics in terms of information flow between the system and the environment is developed, further allowing to define a measure for the degree of non-Markovian behaviour in the open system dynamics.

Another longstanding fundamental question regarding memory effects is their primary origin: What are the properties of the environment, the system and the interaction that cause the evolution to deviate from Markovian dynamics? In research article III the effect of initial correlations between the open system and the environment on the dynamics of the open systems is studied. It is found, that the inability to prepare the system and the environment independently can give rise to pronounced memory effects in the dynamics of the open system. Based on this observation, a scheme for witnessing the initial correlations from the open system dynamics is developed.

The multifaceted nature of the sources of quantum memory effects is accented, when multipartite open systems are studied. For classical stochastic processes a non-Markovian process can always be embedded in a Markovian one by a suitable enlargement of the number of relevant variables. Thus, the general view has been that also for quantum systems enlarging the system under study tunes the dynamics towards a Markovian behaviour. This can indeed be done for certain non-Markovian quantum processes [17–21], but in research article V we see that also the exactly opposite behaviour can occur for quantum systems: enlarging an open quantum system can actually change the dynamics from Markovian to non-Markovian. This is due to nonlocal memory effects, which can occur when the local environments of a bipartite quantum system are initially correlated.

Besides fundamental questions in the heart of the open quantum systems theory, also possible applications in quantum control have been lately

under active research. The possibility to engineer noise processes in open quantum systems is of major importance e.g. in recent proposals for the generation of entangled states [22–24], for dissipative quantum computation [25] and for the enhancement of quantum metrology efficiencies [26]. The environment is usually very complex and thus difficult to control, but nevertheless some sophisticated engineering methods have been developed [27]. In research article IV we report an all-optical experiment in which through selective preparation of the initial environment states we can drive the open system from the Markovian to the non-Markovian regime, control the information flow between the system and the environment, and determine the degree of non-Markovianity. Further, in research article VI, we create memory effects via a careful engineering of frequency correlations between two photons. We observe the nonlocal nature of the memory effects and provide a novel method to experimentally quantify frequency correlations in photonic environments via polarisation measurements.

The introductory part is organised as follows: In chapter 2 the general mathematical framework for open systems and the standard theory of Markovian processes is presented. Further, an introduction to some methods for treating non-Markovian dynamics is given. The characterisation of non-Markovian dynamics in terms of information flow is developed and the concept of nonlocal memory effects is discussed in chapter 3. Chapter 4 addresses the problem of characterising open system dynamics in the presence of initial system environment correlations and finally chapter 5 describes experiments on non-Markovian dynamics in a photonic setup. The final chapter summarises the results of the Thesis.

Chapter 2

Open quantum systems

A closed quantum system with Hilbert space $\mathcal{H}$ and a time independent Hamiltonian operator H, evolves according to the Schrödinger equation, which for a general mixed state $\rho \in \mathcal{S}(\mathcal{H}) = \{\rho \text{ bounded operator on } \mathcal{H} |\ \rho^\dagger = \rho, \rho \geq 0, \mathrm{tr}\,[\rho] = 1\}$ can be written in terms of a unitary operator $U(t) = \exp[-iHt]$:

$$\rho(t) = U(t)\rho U^\dagger(t). \tag{2.1}$$

The unitary dynamics describes fully reversible dynamics, as can be seen from the symmetry: $U(t)^{-1} = U(-t)$. Irreversibility arises when there is an external environment influencing the evolution of the system. Such a quantum system is said to be open and instead of deterministic evolution, its dynamics contains a random element. In the basic construction underlying the theory of open quantum systems one assumes that the environment influencing the dynamics, although having many degrees of freedom, can be described as a quantum system of its own and can thus be represented by a Hilbert space.

Let us denote by $\mathcal{H}_S$ the Hilbert space of the system and by $\mathcal{H}_E$ the Hilbert space of the environment. The Hilbert space of the total system $S + E$ is then given by the tensor product space $\mathcal{H}_S \otimes \mathcal{H}_E$. Now, the full dynamics of the open system and the surrounding environment can be considered closed and the dynamics of the total system is given by Eq. (2.1). The reduced dynamics of the open system S is then obtained by taking a partial trace over the environment degrees of freedom. If at time $t = 0$ the total state is $\rho_{SE}(0) \in \mathcal{S}(\mathcal{H}_S \otimes \mathcal{H}_E)$, then the total state at time t is $\rho_{SE}(t) = U(t)\rho_{SE}(0)U^\dagger(t)$, and

$$\rho_S(t) = \mathrm{tr_E}\left[\mathrm{U(t)}\rho_{\mathrm{SE}}(0)\mathrm{U}^\dagger(\mathrm{t})\right], \tag{2.2}$$

where the partial trace $\mathrm{tr_E}$ is defined via the requirement $\mathrm{tr_{SE}}\left[(\mathrm{A_S}\otimes\mathbb{I})\rho_{\mathrm{SE}}\right] = \mathrm{tr_S}\left[\mathrm{A_S tr_E}\left[\rho_{\mathrm{SE}}\right]\right]$, which has to be valid for all system observables A_S.

In order to introduce the concept of a dynamical map, let us assume that at the initial time $t = 0$ the state of the total system $\rho_{SE}(0)$ can be prepared in an uncorrelated state $\rho_{SE}(0) = \rho_S(0) \otimes \rho_E$, where the environment state ρ_E is fixed. In other words, we assume that the initial state of the system can be prepared independently of the environment[a]. Now, the transformation from an open system state at time $t = 0$ to an open system state at time t can be written as

$$\rho_S(0) \mapsto \rho_S(t) = \Phi_{(t,0)}(\rho_S(0)) = \mathrm{tr_E}\left[\mathrm{U(t)}\rho_{\mathrm{S}}(0) \otimes \rho_{\mathrm{E}}\mathrm{U}^{\dagger}(\mathrm{t})\right]. \tag{2.3}$$

For a fixed time t the map $\Phi_{(t,0)}$ is referred to as a dynamical map, and it is completely positive and trace preserving (CPT), i.e.

(CP) $\Phi_{(t,0)} \otimes \mathbb{I}_n$ is a positive map for all $n \in \mathbb{N}$, where $\mathbb{I}_n$ is the identity operator on the $n \times n$ matrices,

and

(T) $\mathrm{tr}\left[\Phi_{(t,0)}(\rho)\right] = \mathrm{tr}\left[\rho\right]$, for all $\rho \in \mathcal{S}(\mathcal{H})$.

The trace preservation and positivity of the map guarantee that density matrices are mapped to density matrices. The complete positivity means that also any extension of the density matrix on a larger Hilbert space is mapped into a density matrix. It should be noted that the positivity of the map does not imply complete positivity as can be seen for example in the case of a transposition map that is clearly positive but not completely positive. The complete positivity of the dynamical map is generally required as to give a physically reasonable description of the dynamics. But why is positivity of the map not enough to guarantee a physical state transformation? Why is it not sufficient to have physical states as an output for the map? The reason for the necessity of complete positivity arises from the following argument: We cannot exclude a priori that our system S is initially entangled with some distant system M, which does not interact with S. Now, in order for the extended map in $S + M$ to be positive, the map acting in S must be completely positive.

Finding the exact dynamical map is not in general feasible due to the large dimension of total Hilbert space $\mathcal{H}_S \otimes \mathcal{H}_E$ and, in any case, solving the

[a]Later, in chapter 4 of this Thesis, we will also discuss the role of initial correlations between the system and the environment in the dynamics of an open quantum system.

dynamics for the whole system is redundant when we are interested only in a small subsystem with just a few degrees of freedom. Thus, methods for deriving the subsystem dynamics without solving the full time evolution are extremely valuable and many approximative analytical methods [6, 7, 21,28,29] and numerical simulation techniques [30–39] have been developed in recent years for treating open system dynamics efficiently.

2.1 Standard theory of Markovian open quantum sytems

A simple prototype of the dynamics of an open quantum system is given by a Markovian process for which all memory effects are neglected and the dynamics is stationary in time. Then, the family of the dynamical maps $\{\Phi_{(t,0)}\}_{t\geq 0}$ has the semigroup property [5]

$$\Phi_{(t_1+t_2,0)} = \Phi_{(t_2,0)}\Phi_{(t_1,0)}, \quad t_1, t_2 \geq 0. \tag{2.4}$$

Now, for a quantum dynamical semigroup, there exists a generator $\mathcal{L}$ defined as $\Phi_{(t,0)} = \exp[\mathcal{L}t]$ [40] which determines the equation of motion for the reduced density operator:

$$\frac{d}{dt}\rho_S(t) = \mathcal{L}\rho_S(t), \tag{2.5}$$

where $\mathcal{L}$ is an operator acting in $\mathcal{S}(\mathcal{H}_S)$. It has been shown [3, 4], that the most general form of the generator $\mathcal{L}$ is

$$\mathcal{L}\rho_S = -i[H, \rho_S] + \sum_i \gamma_i (A_i \rho_S A_i^\dagger - \frac{1}{2}\{A_i^\dagger A_i, \rho_S\}), \tag{2.6}$$

where H is a Hamiltonian for the system, A_i:s are system operators and $\gamma_i \geq 0$ the corresponding decay rates. Eq. (2.5), with the generator of the form of Eq. (2.6) is often referred to as the Markovian master equation.

Usually, master equations for the subsystem dynamics are either given phenomenologically or derived with microscopic approaches under numerous approximations [6]. However, when many approximations or phenomenological assumptions are made in the derivation, one might end up with an unphysical equation of motion. In this case the dynamical map obtained as the solution to the master equation is not CPT. The power of the mathematical framework of quantum dynamical semigroups lies in the

theorem providing the most general form for the generators of the semigroup. If the generator is of the form of Eq. (2.6), no matter how the master equation was derived, it is always guaranteed that the solution is physically consistent and feasible, i.e. , it gives rise to a family of CP maps. As we will see later on, no such elegant mathematical framework exists for a general, non-Markovian process.

The standard Markov theory has been widely applied (see e.g. [41–45]) and it gives a good qualitative description of many physical systems. However, in the cases of strong system-environment couplings, structured and finite reservoirs, low temperatures, as well as in the presence of large initial system-environment correlations the Markov approximation is no longer valid and other techniques for treating the open system dynamics are needed. In the following we will shortly describe the physical circumstances that allow to perform the Markov approximation.

2.1.1 Microscopic derivation of the Markovian master equation

If the system under interest S and the environment E interact via the Hamiltonian H_I and the total Hamiltonian is of the form $H = H_S + H_E + H_I$, where H_S and H_E are respectively the free Hamiltonians of the system and the environment, the dynamics of the total system is given by the von Neumann equation

$$\frac{d}{dt}\tilde{\rho}(t) = -i\left[H_I(t), \tilde{\rho}(t)\right], \tag{2.7}$$

which is written in the interaction picture, i.e. , $H_I(t) = e^{iH_0 t} H_I e^{-iH_0 t}$, $\tilde{\rho}(t) = e^{iH_0 t}\rho(t)e^{-iH_0 t}$ and $H_0 = H_S + H_E$. A formal integration then gives

$$\tilde{\rho}(t) = \tilde{\rho}(0) - i\int_0^t ds\left[H_I(s), \tilde{\rho}(s)\right]. \tag{2.8}$$

Inserting Eq. (2.8) into Eq. (2.7) and taking the partial trace over the environment allows us to write

$$\frac{d}{dt}\tilde{\rho}_S(t) = -\int_0^t ds \mathrm{tr}_E\left[H_I(t), \left[H_I(s), \tilde{\rho}(s)\right]\right], \tag{2.9}$$

where it is assumed that $\mathrm{tr}_E\left[H_I(t), \tilde{\rho}(0)\right] = 0$. So far, no additional approximations have been performed and Eq. (2.9) describes the dynamics of a general open system. In the microscopic derivation the aim is now to explicitly specify the physical constraints and assumptions that lead to a

Markovian equation of motion of the form given in Eq. (2.6). We will not go through the derivation here in detail, but only briefly summarise the crucial approximations giving rise to a dynamical semigroup. The detailed derivation can be found in e.g. [6].

The first crucial assumption we make is the so called Born approximation, which assumes weak coupling between the system and the environment in such way that the system of interest does not influence the environment during the evolution and thus the total state can be approximated as $\rho(t) \approx \rho_S(t) \otimes \rho_E(0)$. This assumption allows us to write the dynamics in a closed integro-differential form

$$\frac{d}{dt}\tilde{\rho}_S(t) = -\int_0^t ds \mathrm{tr}_E \left[H_I(t), [H_I(s), \tilde{\rho}_S(s) \otimes \rho_E(0)]\right]. \tag{2.10}$$

If we now assume that the dynamics at time t does not explicitly depend on the past states $\rho_S(s)$, $s < t$, we may replace $\rho_S(s)$ in the integrand with $\rho_S(t)$ and the equation of motion can be written in the local in time form

$$\frac{d}{dt}\tilde{\rho}_S(t) = -\int_0^t ds \mathrm{tr}_E \left[H_I(t), [H_I(s), \tilde{\rho}_S(t) \otimes \rho_E(0)]\right], \tag{2.11}$$

which is called the Redfield equation.

Now, in order to obtain a Markovian master equation, we need to take into consideration the relevant time scales of the system under study. Let us denote with τ_E the time scale over which the environment correlation functions decay and with τ_R the time scale over which the system relaxes to a steady state. If we have $\tau_R \gg \tau_E$, the integrand in Eq. (2.11) disappears fast for $s \gg \tau_E$ and thus we can extend the upper limit of integration to infinity and

$$\frac{d}{dt}\tilde{\rho}_S(t) = -\int_0^\infty ds \mathrm{tr}_E \left[H_I(t), [H_I(t-s), \tilde{\rho}_S(t) \otimes \rho_E(0)]\right]. \tag{2.12}$$

This master equation describes the dynamics on a coarse grained time axis where we ignore scales of the order τ_E and focus only on dynamics on the relaxation time scale.

The master equation in Eq. (2.12) is not of the Markovian form of Eq. (2.6) and yet another approximation needs to be performed. This is the so called secular approximation in which an averaging over rapidly oscillating terms in the master equation is performed [6]. The validity of this approximation requires that the timescale of the free evolution of the system τ_S is much smaller than the relaxation time scale τ_R. As a result,

we obtain a master equation of the form in Eq. (2.6) and the evolution is given by a dynamical semigroup.

It should be noted, that also under physical constraints different from what was assumed in the preceding, a Markovian master equation can be derived. For example, in the so called singular coupling limit, where the system and the environment are strongly coupled, a master equation of the form of Eq. (2.6) can be written [6]. Thus, very different physical conditions can lead to a Markovian master equation and no unique physical requirements guaranteeing the semigroup property exist.

2.2 Methods for treating non-Markovian quantum dynamics

The semigroup property given in Eq. (2.4) is a very restricting assumption on the quantum process and, indeed, the approximations performed in the microscopic derivation of the Markovian master equation are often not valid. Thus, open system dynamics is often found to be both non-stationary and non-Markovian. A characterisation of the generators for a general quantum process does not exist, and a great deal of effort has been put into finding generalised master equations for non-Markovian processes. Here, two commonly used master equations for non-Markovian processes are described and their physical validity is discussed. Besides the two approaches presented here, there exists a wide spectrum of techniques for treating open quantum systems (see e.g. [7] and references therein), but it is not in the scope of this thesis to review all of them. We will concentrate only on the following ones, since they are in close connection with one another and all the examples presented in this thesis will be treated within these approaches.

2.2.1 Memory kernel master equations

Memory kernel master equations strive to generalise the Markovian master equation of Eq. (2.5) by introducing a time integration over the past. This has been phenomenologically reasoned to naturally bring about non-Markovian effects. The dynamics is written in the form

$$\frac{d}{dt}\rho_S(t) = \int_0^t dsk(t,s)\rho_S(s), \tag{2.13}$$

where $k(t,s)$ is an operator acting in $\mathcal{S}(\mathcal{H}_S)$. Clearly, the Markovian master equation is obtained for $k(t,s) = \delta(t-s)\mathcal{L}$. However, the general form of $k(t,s)$, such that the subsequent dynamical maps would be CPT is not known, and attempts to derive non-Markovian memory kernel master equations phenomenologically may give unphysical results [46]. Further, even for physically relevant master equations, it has been argued, that sometimes such equations may fail in describing memory effects [47].

However, some forms guaranteeing the physicality of certain memory kernel equations have been derived. In [48] the kernel $k(t,s)$, which is extracted from a reservoir model based on a random telegraph stochastic process, is assumed to be a product of a scalar function with a semigroup generator. For this specific kernel the conditions for the CP property can be derived. Another phenomenological scalar kernel function has been studied in [49] by Shabani and Lidar. The consequent master equation is analytically solvable and the physically relevant parameter region can be identified [50, 51].

There exists also recipes for deriving memory kernel master equations microscopically via the so called projection superoperator methods [52, 53], which allow a systematic perturbation expansion of the dynamics. However, in the superoperator formalism, it is actually possible to eliminate the integration over the past and derive a local in time equation which is in general much more straightforward to solve.

2.2.2 Local in time master equations

Non-Markovian local in time master equations give a relatively simple way to describe memory effects and thus have been widely used to study non-Markovian dynamics [54–58]. They give a generalisation to the Markovian master equation in Eq. (2.5) by allowing time-dependent and temporarily negative decay rates in the generator of Eq. (2.6). The generator of the local in time master equation must, due to the requirements of preservation of Hermiticity and trace of the density matrix, always be of the form

$$\mathcal{L}(t)\rho_S = -i[H,\rho_S] + \sum_i \gamma_i(t)\left(A_i(t)\rho_S A_i^\dagger(t) - \frac{1}{2}\{A_i^\dagger(t)A_i(t),\rho_S\}\right), \tag{2.14}$$

where the decay rates $\gamma_i(t)$ can have temporarily negative values. The negative decay rates arise naturally from the microscopic derivation, when the correlation time of the environment becomes comparable with the relaxation time scale of the system. Interestingly, the negativity of decay rate

does not signify a simple reversal of the direction of the process, but actually encodes the history of the evolution thus allowing memory effects [59].

It has been shown [60, 61] that a memory kernel master equation of Eq. (2.13) can be under fairly general assumptions cast into the time convolutionless form of Eq. (2.14). Even though the local in time description has been introduced already more than thirty years ago and successfully applied to many non-Markovian problems, nevertheless there has been many misunderstandings related to the applicability of these equations [59]. As well as for the memory kernel equations, no theorem for the form of the generator in Eq. (2.14) guaranteeing the complete positivity of the dynamical map exists. It should be noted, that even though the memory kernel and time convolutionless equations are equivalent descriptions of the same dynamics, the local in time description often has some advantages over the memory kernel one. Namely, a local in time differential equation is easier to solve and further, a stochastic unraveling for local in time master equations can be developed [32, 33]. Later on in the next chapter some examples of local in time master equations will be presented and their applicability will be studied.

Chapter 3

Characterising non-Markovian quantum dynamics

In the classical realm Markovian processes are defined via conditional multi-time transition probabilities: When all the multi-time transition probabilities of a process can be expressed as single-time transition probabilities, the process is called Markovian. More explicitly, for a stochastic process taking values in a numerable set $\{x_i\}_{i\in\mathbb{N}}$ the process is called Markovian if the conditional probabilities satisfy the condition

$$p_{1|n}(x_n, t_n|x_{n-1}, t_{n-1}; \ldots; x_0, t_0) = p_{1|1}(x_n, t_n|x_{n-1}, t_{n-1}), \tag{3.1}$$

with $t_n \geq t_{n-1} \geq \cdots \geq t_0$. If the Markov condition is fulfilled, the process can be described solely by giving the equations of motion for the conditional single-time transition probabilities. The equation of motion for the one-point probabilities is referred to as the Chapman-Kolmogorov equation [62].

For quantum systems the hierarchy of n-point probabilities cannot be constructed without explicit reference to a particular choice of measurement scheme. Thus, generalising the classical definition of a Markovian process to the quantum domain is not possible: the criteria for a quantum Markovian process must be constructed from the characteristics of the one-point probabilities, which are obtained from the family of dynamical maps $\{\Phi_{(t,0)}\}_{t\geq 0}$ given in Eq. (2.3).

Due to the difficulty in formulating a Markovianity condition for quantum dynamics, the term "non-Markovianity" has been used quite loosely in the past. Often, the characterisation of memory effects has been based on imprecise arguments on the features of the master equation describing the process. Indeed, the presence of a memory kernel in

the equation of motion has been considered to guarantee non-Markovian dynamics or even being a synonym for it. Further, in the framework of local in time master equations the occurrence of negative decay rates has been identified with non-Markovianity.

However, the master equation depends on the formalism used to derive it, and thus one can not base a rigorous characterisation of the process on the master equation but rather on the family of dynamical maps $\{\Phi_{(t,0)}\}_{t\geq 0}$, which is independent of the formalism used. But, what is really the essence of memory effects in the quantum domain? What is the property of the dynamical process, which defines the occurrence of memory effects? And moreover, what do we even mean by memory effects?

The ambiguity in the treatment of memory effects initiated an endeavour towards a general definition for non-Markovian dynamics. As mentioned earlier, a complete description of memory effects in the quantum domain is problematic and, indeed, there is an ongoing discussion on the exact definition of Markovian dynamics [63–70]. Many interesting approaches to this problem have been proposed and the differences between them have been extensively studied [71]. The measure suggested in Ref. [65] quantifies non-Markovianity in terms of the minimal amount of noise required to make a given quantum channel Markovian. In Ref. [66] Markovian dynamics was identified with the so called divisibility property, i.e. , with the possibility to compose the dynamical map $\Phi_{(t,0)}$ into other CPT maps. In the following section, an approach to the problem in terms of information flow is discussed. This definition for non-Markovian dynamics was developed in papers I and II of this Thesis.

3.1 Information flow in open quantum systems

The early developments in non-Markovian quantum dynamics already embrace the idea of describing memory effects in terms of information flow between the system and the environment. The key argument being that in order for the past states of the system to have an influence on the future dynamics, some earlier lost information must recoil back to the open system. In papers I and II of this thesis the characterisation of memory effects in terms of information flow was formalised and a measure for the degree of non-Markovian behaviour was put forward. In this section the characterisation formalised in papers I and II is presented and some simple examples

of non-Markovian dynamics, partly discussed in paper II, are discussed.

3.1.1 Trace distance

Trace distance is a metric in the state space defined as

$$D(\rho_1, \rho_2) := \frac{1}{2}||\rho_1 - \rho_2||_1, \tag{3.2}$$

where $||A||_1 = \mathrm{tr}\sqrt{\mathrm{AA}^\dagger}$. It can be shown to measure the distinguishability between two quantum states [72]: If a quantum system is prepared in either state ρ_1 or ρ_2, each with probability 1/2, and the goal is to decide in which of the two states the system is in, the quantity $\frac{1}{2}(1 + D(\rho_1, \rho_2))$ gives the optimal probability for successfully identifying the state of the system. If, for example, ρ_1 and ρ_2 are orthogonal, the states can be distinguished with certainty and if, on the other hand, $\rho_1 = \rho_2$ no information of the state can be gained via measurements.

Another desirable property the trace distance enjoys is that CP maps are contractions for D [72]:

$$D(\Phi_t\rho_1, \Phi_t\rho_2) \leq D(\rho_1, \rho_2), \tag{3.3}$$

meaning that quantum operations can never increase the distinguishability between two states. In addition, it is invariant under unitary maps, i.e. , $D(U_t\rho_1 U_t^\dagger, U_t\rho_2 U_t^\dagger) = D(\rho_1, \rho_2)$ and thus for closed systems the distinguishability between states is unchanged in time.

3.1.2 Information flow in terms of trace distance

When the distinguishability between quantum states of the open system changes in time, there is information flowing between the system and the environment. When the distinguishability decreases there are fewer chances to discriminate between the two states. Thus, information has been lost from the system. If, on the other hand, for some interval of time the distinguishability increases, the earlier lost information recoils back to the system. Since the total system including the environment is closed, it evolves according to unitary dynamics and thus there is no information flowing in or out of the total system. Further, the contraction property of Eq. (3.3) guarantees that the maximal amount of information the system can recover is the amount of information lost from the system.

The basic idea underlying the definition for memory effects in a quantum process is that for Markovian processes the information flows continuously from the system to the environment. In order to give rise to non-Markovian effects there must be, for some interval of time, information flowing back to the system. The reasoning being, that the information flowing back to the system allows the earlier sate of the system dynamics to have an effect on the later dynamics of the system, i.e, it allows the occurrence of memory effects.

Since the trace distance is a measure for the distinguishability between quantum states, the information flux in the open system can be quantified via

$$\sigma(t, \rho_{1,2}(0)) = \frac{d}{dt} D(\rho_1(t), \rho_2(t)), \tag{3.4}$$

where $\rho_{1,2}(t) = \Phi(t,0)\rho_{1,2}(0)$. Now, for a non-Markovian process described by a family of dynamical maps $\{\Phi(t,0)\}_{t\geq 0}$, information recoils back to the system for some interval of time and thus we must have $\sigma > 0$ for this time interval. In conclusion, we define Markovian and non-Markovian processes as follows:

- A quantum process $\{\Phi_{(t,0)}\}_{t\geq 0}$ is Markovian, when for all pairs of initial system states $\rho_{1,2}$ and for all times $t \geq 0$ the information flows out from the system, i.e., $\sigma(t, \rho_{1,2}(0)) \leq 0$.

- A quantum process $\{\Phi_{(t,0)}\}_{t\geq 0}$ is non-Markovian, when there exists a pair of initial system states $\rho_{1,2}$ such that for some interval of time the information flows back to the system, i.e., $\sigma(t, \rho_{1,2}(0)) > 0$.

3.2 Measure for the degree of non-Markovian behaviour

Memory effects can manifest themselves in a variety of ways depending on the formalism used and on the physical system under study. In order to compare memory effects between various formalisms one has to develop a quantity determining the degree of non-Markovian behaviour based on the family of dynamical maps. A measure for non-Markovianity based on information flow between the system and the environment can be developed by quantifying the total amount of information flowing back to the system during the evolution. In terms of information flux, defined in Eq. (3.4)

$$\mathcal{N}(\Phi) = \max_{\rho_{1,2}(0)} \int_{\sigma>0} dt \sigma(t, \rho_{1,2}(0)). \tag{3.5}$$

Here, the time integration is extended over all time intervals (a_i, b_i) in which σ is positive and the maximum is taken over all pairs of initial states. The measure does not rely on any specific representation or approximation of the dynamics, nor does it presuppose the existence of a master equation.

3.2.1 Divisible maps

The divisibility property is an extension of the semigroup property given in Eq. (2.4). A dynamical process is called divisible if for all $t \geq 0$ and $\tau \geq 0$ the CPT map $\Phi(\tau + t, 0)$ can be written as composition of the maps $\Phi(\tau + t, t)$ and $\Phi(t, 0)$,

$$\Phi(\tau + t, 0) = \Phi(\tau + t, t)\Phi(t, 0) \tag{3.6}$$

and the maps $\Phi(\tau + t, t)$ and $\Phi(t, 0)$ are CPT. Clearly, a dynamical semigroup is also divisible with the additional property of being time-homogeneous, i.e, $\Phi(t_2, t_1) = \Phi(t_2 - t_1, 0)$. In fact, it is possible to extend the theorem characterising the generators of a semigroup, discussed in section 2.1, for a general divisible process. Namely, one can show that the most general form of a generator of a divisible process can be written in the form given in Eq. (2.14), but with $\gamma_i(t) \geq 0$ for all times.

In Ref. [66] another measure for the non-Markovian character of a process based on the divisibility property was suggested. The measure does not coincide with the one suggested in this Thesis, but there exists a connection between the two approaches. Indeed, due to the contractivity property of Eq. (3.3), for all divisible processes the derivative of trace distance is negative for all times t, i.e., $\sigma(t, \rho_{1,2}(0)) \leq 0$ and therefore $\mathcal{N}(\Phi) = 0$. This further implies that a non-Markovian process is necessarily described by family of dynamical maps which are not divisible. Therefore, one can further conclude that a local in time master equation of the form given in Eq. (2.14) must have at least one negative decay rate in order for it to describe a non-Markovian process.

3.2.2 Some examples

In the following, examples of non-Markovian local in time master equations of the form (2.14) will be presented in order to demonstrate how to determine the measure for non-Markovianity of Eq. (3.5) for some simple quantum processes. The last example furthermore demonstrates that in the presence of multiple decay channels, a process that is not divisible can still have $\mathcal{N}(\Phi) = 0$.

Dynamics with one decay channel

A general amplitude damping channel for a two-level system with excited state $|+\rangle$ and ground state $|-\rangle$ can be described with the master equation

$$\frac{d}{dt}\rho(t) = \gamma(t)(\sigma_-\rho\sigma_+ - \frac{1}{2}\{\sigma_+\sigma_-, \rho\}), \tag{3.7}$$

where $\sigma_- = |-\rangle\langle+|$, $\sigma_+ = |+\rangle\langle-|$ and the decay rate $\gamma(t)$ can take temporarily negative values. Such master equation arises, for example, in the case of a damped Jaynes-Cummings model describing the interaction between a two-level atom and a single cavity mode, which is further coupled to a vacuum bosonic reservoir [6]. For this model a negative decay rate arises in the exact solution, when the coupling between the two-level system and the cavity mode is increased, and consequently, the reservoir correlation time becomes comparable with the system relaxation time scale.

The corresponding dynamical map can be written as

$$\begin{aligned} \rho_{++}(t) &= G(t)^2\rho_{++}(0) \\ \rho_{+-}(t) &= G(t)\rho_{+-}(0) = \rho^*_{-+}(t) \\ \rho_{--}(t) &= \rho_{--}(0) + (1 - G(t)^2)\rho_{++}(0), \end{aligned} \tag{3.8}$$

where $G(t) = \exp[-\Gamma(t)]$, with $\Gamma(t) = \int_0^t \gamma(s)ds$. It can be shown, that the map is CPT if and only if $G(t) \leq 1$, i.e. $\Gamma(t) \geq 0$ and divisible, when $G(t)$ is a monotonically decreasing function [64]. It is also simple to calculate the trace distance for a general pair of states under the evolution of Eq. (3.8): For $A = \rho^1_{++}(0) - \rho^2_{++}(0)$ and $B = \rho^1_{+-}(0) - \rho^2_{+-}(0)$ the trace distance is

$$D(\rho_1(t), \rho_2(t)) = G(t)\sqrt{A^2G(t)^2 + |B|^2}. \tag{3.9}$$

One can easily see from Eq. (3.9) that $\dot{D}$ becomes positive whenever $\dot{G} > 0$ and thus the dynamics becomes non-Markovian whenever $G(t)$ is not monotonically decreasing. Since the divisibility property is equivalent to having only positive decay rates in the time local master equation, for this example, the divisibility condition coincides with the Markovianity condition. To actually determine the value of the measure in Eq. (3.5) is not as straightforward since the pair of states maximising the value of the measure changes depending on the functional form of $G(t)$. Thus the maximising pair for amplitude damping always depends on the specific physical model under study.

Pure dephasing dynamics for a qubit is an example in which the maximisation over the initial pairs of states can be done analytically. A general dephasing process can be described with the master equation

$$\frac{d}{dt}\rho(t) = \frac{\gamma(t)}{2}(\sigma_z\rho\sigma_z - \frac{1}{2}\{\sigma_z\sigma_z, \rho\}), \tag{3.10}$$

where $\sigma_z = |+\rangle\langle+| - |-\rangle\langle-|$. Now, the dynamical map can be written as

$$\begin{aligned} \rho_{++}(t) &= \rho_{++}(0) \\ \rho_{+-}(t) &= G(t)\rho_{+-}(0) = \rho^*_{-+}(t) \\ \rho_{--}(t) &= \rho_{--}(0), \end{aligned} \tag{3.11}$$

with $G(t) = \exp[-\Gamma(t)]$, with $\Gamma(t) = \int_0^t \gamma(s)ds$. Pure dephasing dynamics with a negative decay rate arises, for example, in the context of photonic systems when an interaction between polarisation and energy is generated in a birefringent material. Such system will be studied in more detail in chapter 5 of this Thesis.

As in the case of amplitude damping, the map is CPT if and only if $G(t) \leq 1$, i.e. $\Gamma(t) \geq 0$ and the map is divisible, when $G(t)$ is a monotonically decreasing function. The trace distance is

$$D(\rho_1(t), \rho_2(t)) = \sqrt{A^2 + |B|^2 G(t)^2}, \tag{3.12}$$

and thus the dynamics becomes non-Markovian again whenever $G(t)$ is not monotonically decreasing, i.e. $\gamma(t) < 0$. Now, for the dephasing dynamics, we see that the pair maximising the increase of the trace distance (3.12) is such that $A = 0$ and $|B| = 1$, independent of the functional form of $G(t)$. Thus the measure for a general dephasing process can be written as

$$\mathcal{N}(\Phi) = \int_{\dot{G}>0} \dot{G}(t)dt. \tag{3.13}$$

From the preceding examples one can clearly see that the emergence of non-Markovian dynamics is related to the negativity of the decay rates in the time local master equation. However, this is not a general feature but only a consequence of having just one decay channel. Moreover, in the case of one decay channel the divisibility and Markovianity are equivalent properties. In the following example, instead, the multiple decay channels present in the master equation bring about dynamics, where the Markovianity of the map does not guarantee the divisibility of the channel and thus having one negative decay rate does not suffice to generate memory effects.

Dynamics with multiple decay channels

A generalised amplitude damping model with two decay channels can be described via the master equation

$$\begin{aligned}\frac{d}{dt}\rho(t) &= \gamma_-(t)(\sigma_-\rho\sigma_+ - \frac{1}{2}\{\sigma_+\sigma_-,\rho\}) \\ &\quad +\gamma_+(t)(\sigma_+\rho\sigma_- - \frac{1}{2}\{\sigma_-\sigma_+,\rho\}),\end{aligned} \tag{3.14}$$

which generates the map

$$\begin{aligned}\rho_{++}(t) &= (\alpha(t)^2+\beta(t))\rho_{++}(0)+\beta(t)\rho_{--}(0) \\ \rho_{+-}(t) &= \alpha(t)\rho_{+-}(0)=\rho^*_{-+}(t) \\ \rho_{--}(t) &= (1-\alpha(t)^2-\beta(t))\rho_{++}(0)+(1-\beta(t))\rho_{--}(0),\end{aligned} \tag{3.15}$$

where $\alpha(t) = \exp\left[-\frac{1}{2}\Gamma_\pm(t)\right]$, $\beta(t) = \exp\left[-\Gamma_\pm(t)\right]\int_0^t \gamma_+(s)\exp\left[\Gamma_\pm(s)\right]ds$ and $\Gamma_\pm(t) = \int_0^t(\gamma_+(s)+\gamma_-(s))ds$. The map (3.15) is CPT if and only if $\beta(t)\geq 0$ and $\alpha(t)^2+\beta(t)\leq 1$. Now, the trace distance can be written as

$$D(\rho_1(t),\rho_2(t)) = \alpha(t)\sqrt{A^2\alpha(t)^2+|B|^2}, \tag{3.16}$$

which is of the same form as the trace distance for the amplitude damping with one decay channel in Eq. (3.9). However, the trace distance now increases, if and only if $\gamma_+(t)+\gamma_-(t)\leq 0$ for some interval of time. Thus, in order for the process to be non-Markovian it is not enough to have only one of the decay rates negative. On the contrary, the divisibility property breaks down, whenever at least one of the decay rates becomes negative.

3.3 Nonlocal memory effects

In the preceding chapter all the examples were developed around the dynamics of a single qubit. In fact, a far more interesting situation occurs, when the system under study is bipartite. The following theory for bipartite systems was developed in paper V of this Thesis, where a hitherto unexplored source for memory effects was introduced. Namely, it was found that initial correlations between the environments of a bipartite system can generate a nonlocal process from a local interaction Hamiltonian and, further, that the nonlocal dephasing process can exhibit memory effects although the local dynamics is Markovian.

Let us consider a generic scenario, where there are two systems, labeled with indices $i = 1, 2$, which interact locally with their respective environments. The dynamics of the two systems can be described via the equation

$$\begin{aligned} \rho_S^{12}(t) &= \Phi_{12}(t)(\rho_S^{12}(0)) \\ &= \mathrm{tr}_E \left[\left(U_{SE}^{1t} \otimes U_{SE}^{2t} \right) \rho_S^{12}(0) \otimes \rho_E^{12}(0) \left(U_{SE}^{1t\dagger} \otimes U_{SE}^{2t\dagger} \right) \right], \end{aligned} \tag{3.17}$$

where U_{SE}^{it} is the local unitary operator describing the interaction between the system i and its environment. Now, if the initial environment state $\rho_E^{12}(0)$ is factorized, i.e. , $\rho_E^{12}(0) = \rho_E^1(0) \otimes \rho_E^2(0)$, also the map $\Phi_{12}(t)$ factorizes. Thus, the dynamics of the two systems is given by a local map $\Phi_{12}(t) = \Phi_1(t) \otimes \Phi_2(t)$. On the other hand, if $\rho_E^{12}(0)$ exhibits correlations, the map $\Phi_{12}(t)$ can not, in general, be factorized. Consequently, the environmental correlations may give rise to a nonlocal process even though the interaction Hamiltonian is purely local.

For a local dynamical process, all the dynamical properties of the subsystems are inherited by the global system, but naturally for a nonlocal process the global dynamics can display characteristics absent in the dynamics of the local constituents. Especially, for a nonlocal process, even if the subsystems undergo a Markovian evolution, the global dynamics can nevertheless be highly non-Markovian as will be shown for the dephasing model presented in the following.

3.3.1 General dephasing model with initial correlations between the environments

A general dephasing map for two qubits can be written as

$$\rho_{12}(t) = \begin{pmatrix} |a|^2 & ab^*\kappa_2(t) & ac^*\kappa_1(t) & ad^*\kappa_{12}(t) \\ ba^*\kappa_2^*(t) & |b|^2 & bc^*\Lambda_{12}(t) & bd^*\kappa_1(t) \\ ca^*\kappa_1^*(t) & cb^*\Lambda_{12}^*(t) & |c|^2 & cd^*\kappa_2(t) \\ da^*\kappa_{12}^*(t) & db^*\kappa_1^*(t) & dc^*\kappa_2^*(t) & |d|^2 \end{pmatrix}, \tag{3.18}$$

where the initial state of the two qubits is a pure state

$$|\psi_{12}\rangle = a\,|00\rangle + b\,|01\rangle + c\,|10\rangle + d\,|11\rangle\,. \tag{3.19}$$

It can be easily seen, that the dynamics of the subsystems, $\rho_1(t) = \mathrm{tr}_2\left[\rho_{12}(t)\right]$ and $\rho_2(t) = \mathrm{tr}_1\left[\rho_{12}(t)\right]$, are determined solely by the functions $\kappa_1(t)$ and $\kappa_2(t)$ and depend on neither $\kappa_{12}(t)$ nor $\Lambda_{12}(t)$. Thus, the map

given by Eq. (3.18) does not factorize in general, i.e. , it produces a nonlocal process.

As a specific physical system we take a model of two qubits interacting with correlated multimode bosonic fields [73]. The qubits interact locally with their respective environments via the interaction Hamiltonians $H_i = \sum_k \sigma_z^i (g_k b_k^{i\dagger} + g_k^* b_k^i)$, where we have assumed that the interaction strengths in both systems are identical, i.e. , $g_k^1 = g_k^2 = g_k$. Now, we take the total interaction Hamiltonian to be of the form $H_{\rm INT}(t) = \chi_1(t)H_1 + \chi_2(t)H_2$, where the function $\chi_i(t)$ is 1 for $t_i^{\rm s} \leq t \leq t_i^{\rm f}$ and zero otherwise. Here, $t_i^{\rm s}$ and $t_i^{\rm f}$ denote the times the interaction is switched on and switched off in system i, respectively.

Since the local Hamiltonians H_i commute, the time evolution of the total system is given by $|\Psi(t)\rangle = \exp\left[-i\int_0^t dt' H_{\rm INT}(t')\right]|\Psi(0)\rangle$, where $|\Psi\rangle$ is the state of the total system. We will further denote the local interaction times as $t_i(t) = \int_0^t \chi_i(t')dt'$ and for convenience we will not explicitly write the time dependence of t_i. Now, the local time-evolution of the systems is given by the unitary oprator

$$U_i(t) = \exp\left\{\sigma_z^i \sum_k (b_k^{i\dagger}\xi_k(t_i) - b_k^i \xi_k^*(t_i))\right\}, \tag{3.20}$$

where

$$\xi_k(t_i) = g_k \frac{1 - e^{-i\omega_k t_i}}{\omega_k} \tag{3.21}$$

and the total system evolves under unitary dynamics $U_{12}(t) = U_1(t) \otimes U_2(t)$. The local unitary operator of Eq. (3.20) acts in the following way:

$$\begin{aligned} U_i(t)\,|0\rangle \otimes |\psi\rangle &= |0\rangle \otimes \bigotimes_k D(-\xi_k(t_i))\,|\psi\rangle\,, \\ U_i(t)\,|1\rangle \otimes |\psi\rangle &= |1\rangle \otimes \bigotimes_k D(\xi_k(t_i))\,|\psi\rangle\,, \end{aligned} \tag{3.22}$$

where $D(x_k)$ is the displacement operator for the kth mode.

Let us take as the initial state $|\psi(0)\rangle = |\psi_{12}\rangle \otimes |\eta_{12}\rangle$, where $|\psi_{12}\rangle$ is given by Eq. (3.19) and $|\eta_{12}\rangle = \bigotimes_k |\eta_{12}^k\rangle$. Now the decoherence process is given by Eq. (3.18), where the functions are defined as $\kappa_1(t) = {\rm Tr}\,|\eta_{12}^{00}\rangle\langle\eta_{12}^{10}|$, $\kappa_2(t) = {\rm Tr}\,|\eta_{12}^{00}\rangle\langle\eta_{12}^{01}|$, $\kappa_{12}(t) = {\rm Tr}\,|\eta_{12}^{00}\rangle\langle\eta_{12}^{11}|$, $\Lambda_{12}(t) = {\rm Tr}\,|\eta_{12}^{01}\rangle\langle\eta_{12}^{10}|$ and

$$|\eta_{12}^{xy}(t)\rangle = \bigotimes_k \left[D((-1)^x\xi_k(t_1)) \otimes D((-1)^y\xi_k(t_2))\right]|\eta_{12}\rangle\,. \tag{3.23}$$

After some algebra, one finds

$$\begin{aligned}
\kappa_1(t) &= \prod_k \chi_k(-2\xi_k(t_A), 0), \\
\kappa_2(t) &= \prod_k \chi_k(0, -2\xi_k(t_B)), \\
\kappa_{12}(t) &= \prod_k \chi_k(-2\xi_k(t_A), -2\xi_k(t_B)), \\
\Lambda_{12}(t) &= \prod_k \chi_k(-2\xi_k(t_A), 2\xi_k(t_B)),
\end{aligned} \tag{3.24}$$

where $\chi_k(x, y)$ is the characteristic function of the state $\left|\eta^k_{AB}\right\rangle$.

We will consider a two-mode Gaussian state with the characteristic function $\chi_k(x, y) = \chi_k(\lambda_1, \lambda_2, \lambda_3, \lambda_4) = \exp(-\frac{1}{2}\vec{\lambda}^T \boldsymbol{\sigma} \vec{\lambda})$, where $\lambda_1 = \Re[x]$, $\lambda_2 = \Im[x]$, $\lambda_3 = \Re[y]$, $\lambda_4 = \Im[y]$ and

$$\boldsymbol{\sigma} = \begin{pmatrix} A & C \\ C^T & B \end{pmatrix},$$

is the covariance matrix of the state. Let us take $A = B = \mathbb{I}$ and $C = c\mathbb{I}$. Now, the state is uncorrelated if and only if $c = 0$. We can write

$$\chi_k(x, y) = \exp\left[-\frac{1}{2}\left\{|x|^2 + |y|^2 + c(xy^* + x^*y)\right\}\right]. \tag{3.25}$$

For $c = -1$ we get $\chi_k(x, y) = \exp\left[-\frac{1}{2}|x - y|^2\right]$ and $\kappa_{12}(t) = \exp\left[-2\sum_k |\xi_k(t_1) - \xi_k(t_2)|^2\right]$, where ξ_k is given in Eq. (3.21). Going to the continuous limit of modes we get

$$\kappa_{12}(t) = \exp\left\{-4\int_0^\infty J(\omega)\frac{1 - \cos\left[\omega|t_1(t) - t_2(t)|\right]}{\omega^2}\right\},$$

where $J(\omega)$ is the spectral function of the reservoir. For an Ohmic spectral function $J(\omega) = \alpha\omega\exp(-\omega/\omega_c)$, with α the coupling constant and ω_c a cutoff frequency, we have

$$\begin{aligned}
\kappa_1(t) &= \left(1 + \omega_c^2 t_1(t)^2\right)^{-2\alpha}, \\
\kappa_2(t) &= \left(1 + \omega_c^2 t_2(t)^2\right)^{-2\alpha}, \\
\kappa_{12}(t) &= \left(1 + \omega_c^2 |t_1(t) - t_2(t)|^2\right)^{-2\alpha}, \\
\Lambda_{12}(t) &= \kappa_1^2(t)\kappa_2^2(t)/\kappa_{12}(t).
\end{aligned} \tag{3.26}$$

3.3.2 Nonlocal memory effects in the dephasing dynamics

Let us now examine the information flow between the bipartite system and the environment. We choose a pair of initial states for the bipartite system: $|\psi_{1,2}(0)\rangle = \frac{1}{\sqrt{2}}(|00\rangle \pm |11\rangle)$. For this pair of states the time evolution of the trace distance in Eq. (3.3) has a simple form $D(\rho_1(t), \rho_2(t)) = |\kappa_{12}(t)|$, where $\kappa_{12}(t)$ is given by Eq. (3.26). Now, for the subsystems 1 and 2 the dynamics can be described with a simple dephasing map of Eq. (3.11). Thus, for the individual qubits we know the maximising pairs of states and can thus deduce analytically the non-Markovianity measure. The trace distance for the maximising pair in system 1 is given by $D_1(t) = |\kappa_1(t)|$ and in system 2 $D_2(t) = |\kappa_2(t)|$. Now the trace distance dynamics in systems 1, 2 as well as the global dynamics are presented in Fig. 3.1 for different values of the parameter c describing the strength of the correlations between the environment states. One can clearly see that the trace distance in the subsystems 1 and 2 continuously decreases, but for the total system the trace distance does indeed increase: we obtain dynamics which is locally Markovian but globally exhibits memory effects.

From this example we can conclude that a system can globally recover its earlier lost quantum properties although the constituent parts are undergoing decoherence. This is possible, because the correlations in the initial state of environment give rise to nonlocal dynamics, where an otherwise destructive local interaction is harnessed to create strong memory effects, which allow the system to recover its quantum properties globally. In this way initial environmental correlations can diminish the otherwise destructive effects of decoherence.[a]

[a]The author became aware of a mistake in the calculation (in Eqs. (3.21)-(3.26)) after submitting the Thesis. Steffen Wissmann found the error and derived the corrected equations. He did not give the permission to cite his unpublished material in this Thesis and therefore, the error is unfortunately not fixed here. However, with the corrected calculations a plot qualitatively the same with Fig. 3.1 can be produced and the conclusions are unchanged.

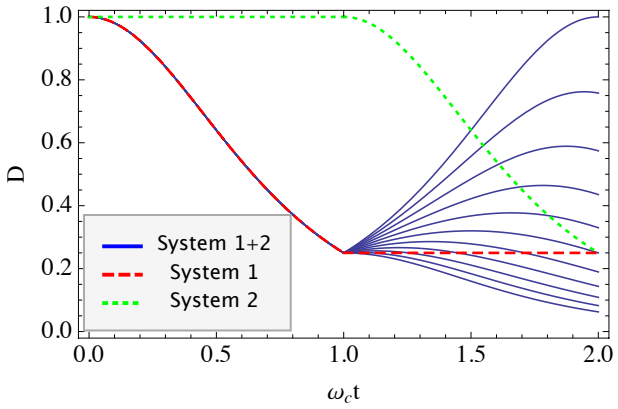

Figure 3.1: The trace distance dynamics for the two qubits interacting with correlated multimode fields. We take $\alpha = 1$, $t_1^s = 0$, $t_1^f = 0 = t_2^s$ and $t_2^f = 2$. The blue lines represent the trace distance with different values of c for the global dynamics of the two qubits for the pair of initial states $|\psi_{1,2}(0)\rangle = \frac{1}{\sqrt{2}}(|00\rangle \pm |11\rangle)$. The maximal increase is obtained for $c = -1$. The dashed red line and the dotted green line give the trace distance evolution for the initial states $1/\sqrt{2}(|0\rangle \pm |1\rangle)$ in systems 1 and 2, respectively.

Chapter 4

The role of initial system-environment correlations in open system dynamics

When the initial state of an open quantum system can be prepared independently from its environment, the evolution of the reduced system can be described by a family of completely positive dynamical maps. The assumption of initially uncorrelated states is well justified in many physical systems, but it has been argued [74], that in general, it is too restrictive and thus the influence of initial correlations on the open system dynamics has been under an active discussion in recent years [74–81].

If one takes into account the possibility of system-environment correlations in the initial states of the total system, the reduced system dynamics can not in general be described by a dynamical map [74, 75, 77]. Such a situation occurs, when it is not possible to prepare the system and the environment independent of one another, due to e.g. a prior interaction between them. Initial correlations can potentially be relevant in various physical systems, and thus the following question arises: When the standard description for open systems is not possible, can one yet find general quantitative features that characterise the reduced system dynamics? In this chapter, the issue of describing open systems with initial correlations in terms of CP maps will be discussed and an approach in terms of information flow, developed in paper III of this Thesis, is presented. Based on the description in terms of information flow, in line with paper III of this thesis, a scheme for witnessing the correlations is presented and an example of a spin-star model is put forward.

4.1 The problem of characterising initially correlated open systems

In chapter 2 the theory of open systems was developed for uncorrelated initial system-environment states, for which, the dynamics can be formulated in terms of completely positive dynamical maps. In the standard approach to initially correlated open quantum systems the aim is to determine under which conditions the system dynamics, given by Eq. (2.2), can be described with CP maps even in the presence of initial correlations. The problem can be formalised as follows.

Assume that the system-environment initial states can not be arbitrarily chosen from the state space $\mathcal{S}(\mathcal{H}_S \otimes \mathcal{H}_E)$, but the available states are determined by some physical constraints on the environment state or on the correlations the system and the environment share. Let us denote the set of available states by the subset $\Omega_{SE} \subset \mathcal{S}(\mathcal{H}_S \otimes \mathcal{H}_E)$. Now, one can ask, what are the conditions on Ω_{SE} that allow to write the dynamics as a family of CP maps [82]. The problem is presented in a pictorial form in Fig. 4.1. Naturally, in the absence of initial correlations $\Omega_{SE} = \{\rho_S(0) \otimes \rho_E |\, \rho_S(0) \in \mathcal{S}(\mathcal{H}_S), \rho_E \text{ fixed}\}$ and the dynamics can be described by CP maps. On the contrary, for an arbitrary Ω_{SE} the dynamics can not by any means be described by a map acting on the open systems state space, since e.g. two different total system states with the same reduced states may evolve in time into states with different reduced system states [74, 75, 77]. Indeed, no generally acknowledged answer to this question has been found and there is a vivid ongoing debate on the topic [81–83].

Another possible approach to initially correlated open systems is to include the process of system state preparation in the description [84, 85]. When the preparation process is taken into account explicitly, the dynamics can be described in terms of CP maps, even in the presence of initial correlations between the system and the environment. However, the CP map does not act in the whole state space of the system but on the possible system preparations [85].

In the following we present yet another approach, in which the information flow between the system and the environment is studied. The approach is fully general, since the initial correlations are not of any specific type, i.e. , no assumptions on Ω_{SE} are made.

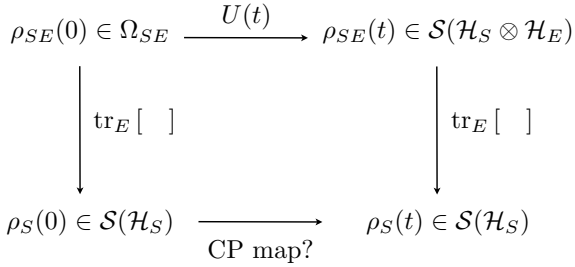

Figure 4.1: A schematic picture of the problem of describing open system dynamics in the presence of initial correlations. For which Ω_{SE} does a completely positive map describe the open system dynamics?

4.2 Bounds for information flow in the presence of initial correlations

When the system and the environment are initially uncorrelated and the environmental state is fixed ρ_E, i.e. , $\rho_{SE} = \rho_S \otimes \rho_E$, one can describe the time evolution of the reduced system given by Eq. (2.3) through a family of completely positive dynamical maps $\Phi_t : \rho_S(0) \mapsto \rho_S(t)$. It is a well known fact [72] that such dynamical maps are contractions for the trace distance, as written previously in Eq. (3.3). Hence, for initially uncorrelated total system states and a fixed environment state, the trace distance between the reduced system states at time t can never be larger than the trace distance between the initial states. Physically this means that the total amount of the information flowing back from the environment to the system is bounded from above by the amount of the information earlier flowed out from the system since the initial time.

As discussed earlier, in the presence of initial correlations the dynamics of the reduced system can no longer be described by a map acting on the state space of the system. However, the time derivative of the trace distance given in Eq. (3.4) can be still interpreted as the flow of information between the system and the environment. But now, if initial correlations are present Eq. (3.3) does not apply and a situation where the trace distance of the reduced system states grows to values which are larger than the initial trace distance can occur. Thus, the initial correlations between the system

and the environment allow the information to flow to the system, even at the initial time (see Fig. 4.2). But how much information can flow to the system, if there are initial correlations present? Can we somehow generalise the contractivity property for initially correlated systems? It turns out that more general bounds for the information flow do exist. In the following, we will derive these bounds and discuss their physical implications.

Now, the aim is to construct an upper bound for the growth of the trace distance in the presence of initial correlations. We consider an arbitrary pair of initial states $\rho_{SE}^{(1),(2)}$ of the total system with the corresponding reduced system states $\rho_S^{(1),(2)} = \mathrm{tr}_E\big[\rho_{SE}^{(1),(2)}\big]$ and environment states $\rho_E^{(1),(2)} = \mathrm{tr}_S\big[\rho_{SE}^{(1),(2)}\big]$. One can derive the inequality

$$\begin{aligned} &D\left(\mathrm{tr}_E\big[U_t\rho_{SE}^{(1)}U_t^\dagger\big], \mathrm{tr}_E\big[U_t\rho_{SE}^{(2)}U_t^\dagger\big]\right) - D(\rho_S^{(1)}, \rho_S^{(2)}) \\ &\leq D(\rho_{SE}^{(1)}, \rho_{SE}^{(2)}) - D(\rho_S^{(1)}, \rho_S^{(2)}) \equiv I(\rho_{SE}^{(1)}, \rho_{SE}^{(2)}), \end{aligned} \tag{4.1}$$

which is a generalisation of the contractivity property. Indeed, for uncorrelated initial states and a fixed environment state, one obtains the usual bound of Eq. (3.4). The inequality states that the increase of the trace distance between $\rho_S^{(1)}$ and $\rho_S^{(2)}$ during the time evolution is bounded from above by the quantity $I(\rho_{SE}^{(1)}, \rho_{SE}^{(2)})$, which represents the loss of distinguishability of the initial total states resulting when measurements on the reduced system only can be performed. One can thus interpret $I(\rho_{SE}^{(1)}, \rho_{SE}^{(2)})$ as the information which lies initially outside the open system and is inaccessible for it. The inequality (4.1) therefore leads to the following physical interpretation: The maximal amount of information the open system can gain from the environment is the amount of information flowed out earlier from the system since the initial time, plus the information which is initially outside the open system.

An important special case of the inequality (4.1) revealing most clearly the role of initial correlations, is obtained when $\rho_{SE}^{(2)}$ is chosen to be the fully uncorrelated state constructed from the marginals of $\rho_{SE}^{(1)}$, i.e. , $\rho_{SE}^{(2)} = \rho_S^{(1)} \otimes \rho_E^{(1)}$. In this case inequality (4.1) simplifies to

$$D\left(\mathrm{tr}_E\big[U_t\rho_{SE}^{(1)}U_t^\dagger\big], \mathrm{tr}_E\big[U_t\rho_S^{(1)} \otimes \rho_E^{(1)}U_t^\dagger\big]\right) \leq D(\rho_{SE}^{(1)}, \rho_S^{(1)} \otimes \rho_E^{(1)}). \tag{4.2}$$

This inequality shows how far from each other two initially indistinguishable reduced states can evolve when only one of the two total initial states is correlated. The upper bound of inequality (4.2) describes how well the state

$\rho_{SE}^{(1)}$ can be distinguished from the corresponding fully uncorrelated state $\rho_S^{(1)} \otimes \rho_E^{(1)}$ and, therefore, provides a measure for the amount of correlations in the state $\rho_{SE}^{(1)}$. Thus, the increase of the trace distance is bounded from above by the correlations in the initial state.

Returning to the general case described with inequality (4.1) and further applying the subadditivity of the trace distance with respect to tensor products results into the inequality

$$\begin{aligned} & D\left(\mathrm{tr}_E\big[U_t \rho_{SE}^{(1)} U_t^\dagger\big], \mathrm{tr}_E\big[U_t \rho_{SE}^{(2)} U_t^\dagger\big]\right) - D(\rho_S^{(1)}, \rho_S^{(2)}) \\ & \leq D(\rho_{SE}^{(1)}, \rho_{SE}^{(2)}) - D(\rho_S^{(1)} \otimes \rho_E^{(1)}, \rho_S^{(2)} \otimes \rho_E^{(2)}) + D(\rho_E^{(1)}, \rho_E^{(2)}) \\ & \leq D(\rho_{SE}^{(1)}, \rho_S^{(1)} \otimes \rho_E^{(1)}) + D(\rho_{SE}^{(2)}, \rho_S^{(2)} \otimes \rho_E^{(2)}) + D(\rho_E^{(1)}, \rho_E^{(2)}), \end{aligned} \tag{4.3}$$

where the second inequality follows by using twice the triangle inequality. This inequality clearly shows that in the most general case an increase of the trace distance of the reduced states implies that there are initial correlations in $\rho_{SE}^{(1)}$ or $\rho_{SE}^{(2)}$, or that the initial environmental states are different. Thus for identical environmental states any increase of the trace distance is a witness for the presence of initial correlations.

4.3 Witnessing initial correlations via information flow

How can one use the above results to develop experimental methods for the detection of correlations in an unknown initial state $\rho_{SE}^{(1)}$? In order to do this, one has to be able to perform a state tomography on the open system at the initial time zero and at some later time t in order to determine the reduced states $\rho_S^{(1)}(0) = \mathrm{tr}_E\big[\rho_{SE}^{(1)}\big]$ and $\rho_S^{(1)}(t) = \mathrm{tr}_E\big[U_t \rho_{SE}^{(1)} U_t^\dagger\big]$. To detect initial correlations by applying inequality (4.3) we need to be able to provide a reference state $\rho_{SE}^{(2)}$ which has the same environmental state as $\rho_{SE}^{(1)}$, i.e. , $\rho_E^{(1)} = \rho_E^{(2)}$. This can be achieved by performing a local trace-preserving quantum operation on $\rho_{SE}^{(1)}$ to obtain the state $\rho_{SE}^{(2)} = (\mathcal{S} \otimes I)\rho_{SE}^{(1)}$. Now, since $\rho_{SE}^{(2)}$ is obtained from $\rho_{SE}^{(1)}$ via a local operation, it is clear that it can be correlated only if $\rho_{SE}^{(1)}$ is correlated. Thus, if the trace distance at any time t increases above its initial value, $D\big(\rho_S^{(1)}(t), \rho_S^{(2)}(t)\big) > D(\rho_S^{(1)}(0), \rho_S^{(2)}(0))$, the inequality (4.3) implies that the original system-environment state $\rho_{SE}^{(1)}$ was correlated.

In order to apply this strategy for detecting initial correlations only local control and measurements of the open quantum system are needed. No knowledge of the structure of the environment or of the system-environment interaction is needed, nor a full knowledge of the initial system-environment state $\rho_{SE}^{(1)}$. Moreover, there is no restriction on the operation $\mathcal{S}$ used to generate the reference state $\rho_{SE}^{(2)}$, which opens a large number of possible experimental realisations. Indeed, this scheme for detecting initial correlations has been successfully applied experimentally for photonic systems with various type of initial correlations [86, 87]. Further, also a scheme for detecting quantum discord by measuring information flow was developed in [88].

4.3.1 Initial correlations in the spin-star model

We study a central spin with Pauli operator σ interacting with a bath of N identical spins with Pauli operators $\sigma^{(k)}$ through the Hamiltonian

$$H = A_0 \sum_{k=1}^{N} (\sigma_+ \sigma_-^{(k)} + \sigma_- \sigma_+^{(k)}). \tag{4.4}$$

Let us assume, that we have a highly correlated state between the system and the environment

$$\rho_{SE}^{(1)} = |\Psi\rangle\langle\Psi|, \quad |\Psi\rangle = \alpha\,|-\rangle \otimes |\chi_+\rangle + \beta\,|+\rangle \otimes |\chi_-\rangle\,, \tag{4.5}$$

where $|\pm\rangle$ are central spin states, and $|\chi_+\rangle = |++\cdots+\rangle$ and $|\chi_-\rangle = \frac{i}{\sqrt{N}} \sum_k |k\rangle$ are environment states. The state $|k\rangle$ is obtained from $|\chi_+\rangle$ by flipping the kth bath spin. The aim is to detect the initial correlations by performing local operations and measurements on the central spin only.

A non-selective measurement of the z-component of the central spin will produce the state

$$\rho_{SE}^{(2)} = |\alpha|^2\,|-\rangle\langle-| \otimes |\chi_+\rangle\langle\chi_+| + |\beta|^2\,|+\rangle\langle+| \otimes |\chi_-\rangle\langle\chi_-|\,. \tag{4.6}$$

Now, we compare the reduced dynamics of this state with $\rho_S^{(1)}(t)$. We find that the increase of the trace distance is given by

$$D\left(\mathrm{tr}_E\left[U_t \rho_{SE}^{(1)} U_t^\dagger\right], \mathrm{tr}_E\left[U_t \rho_{SE}^{(2)} U_t^\dagger\right]\right) = |\Re(\alpha^*\beta)\sin(2At)|, \tag{4.7}$$

where $A = \sqrt{N} A_0$. The trace distance thus oscillates periodically between the initial value zero and the maximal value $|\Re(\alpha^*\beta)|$. Clearly, the contraction property in Eq.(3.2) is not fulfilled and the evolution is not given

by dynamical map. We conclude that for almost all values of the amplitudes α and β there is an increase of the trace distance witnessing the initial correlations. Moreover, we have $D(\rho_{SE}^{(1)}, \rho_{SE}^{(2)}) = |\alpha\beta|$. Hence, if $\alpha^*\beta$ is real the upper bound of inequality (4.1) is reached periodically whenever $|\sin(2At)| = 1$, as is shown in Fig. 4.2 for the case $\alpha = \beta = 1/\sqrt{2}$.

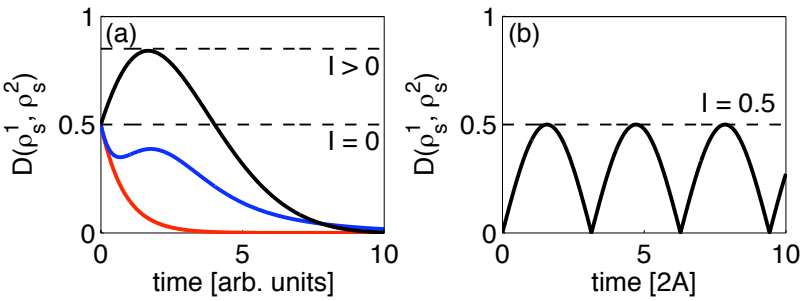

Figure 4.2: (a) Schematic picture of the dynamics of the trace distance. For $I(\rho_{SE}^{(1)}, \rho_{SE}^{(2)}) = 0$ the trace distance may decrease monotonically according to a Markovian dynamics [red line], or may show a non-monotonic behavior in the non-Markovian case [blue line], but can never exceed the initial value marked by the lower dashed line. The black curve illustrates the dynamics in a case with $I(\rho_{SE}^{(1)}, \rho_{SE}^{(2)}) > 0$ for which initially inaccessible information allows the increase of the trace distance over the initial value. The bound of Eq. (4.1) is indicated by the upper dashed line. (b) Example of the exact trace distance dynamics of the reduced system states for the spin-bath model.

Chapter 5

From theory to experiments: Non-Markovian dynamics in photonic systems

In the framework of open quantum systems, the environment is in general composed of a large number of uncontrollable degrees of freedom. Still, as the control over the experimental systems has advanced, some sophisticated schemes for modifying the environment have been developed [27]. Physical systems for which robust schemes for noise engineering can be developed are crucial for modern day quantum control [22–26] and thus extensively studied.

Quantum optics experiments have been the bedrock for testing fundamental paradigms of quantum mechanics. Indeed, the first proof of principle experiments on e.g. quantum interference phenomena [89–91], Bell's theorem [92–94], quantum teleportation [95–97] and quantum contextuality [98, 99] have been performed with optical setups. The appeal for using photonic systems arises from the extremely high control over the degrees of freedom which makes it also an ideal candidate for the physical realisation of communicating and storing quantum information or for quantum computing. In addition, in optical setups entanglement is an accessible resource, almost routinely produced in a modern optics lab with spontaneous parametric downconversion (SPDC).

In an all optical setup, a controlled interaction between different degrees of freedom of a photon can be generated and the initial environmental states can be selectively prepared. The photons, which are created with SPDC, can be prepared in arbitrary polarisation states and a full state tomography

is feasible. Thus, a photonic setup offers an optimal platform for studying fundamental aspects of open quantum systems in a controlled fashion.

In the following, the main results of the experiments reported in papers IV and VI of this Thesis on non-Markovian quantum systems are presented. Besides the ones displayed here, a series of other experimental studies on non-Markovian dynamics in photonic systems have been performed recently. In [100] the non-Markovianity of a process with controllable system-environment interaction is measured, in [101] controllable entanglement oscillations in an effective non-Markovian channel are observed and in [102] non-Markovian dynamics is simulated in a linear optics setup. Before the results of the experiments in papers IV and VI are presented, we will go through the physical basis of the key elements used in both setups.

5.1 Basic elements of the experimental setups

In the framework of open quantum systems, the system and the environment are defined as two sets of degrees of freedom, which can be prepared independently prior to interaction. In the photonic setups under study here these two degrees of freedom are not spatially separated, but are actually different degrees of freedom of a single photon. In the experiments presented in papers IV and VI the interaction is induced in a quartz plate, which couples the polarisation of the photon with its frequency. Thus, the open system will be the polarisation degree of freedom with the Hilbert space $\mathcal{H}_S = \text{span}\{|H\rangle, |V\rangle\}$ and the environment the frequency degree of freedom with $\mathcal{H}_E = \text{span}\{|\omega\rangle\}_\omega$.

Both the experiments presented here consist of three parts: state preparation, interaction and state tomography. In the following a description of the experimental realisation of these three parts will be discussed. First, the preparation of polarisation states of photon pairs created in SPDC sources is reviewed. Then the theoretical description of the decoherence process induced by a quartz plate is given, and finally, the experimental realisation of state tomography of polarisation states is discussed.

5.1.1 Bright sources of entangled photon pairs and state preparation

In the two experiments the photons are created with SPDC. In paper IV both factorized and entangled photon pairs are needed and thus type I SPDC is used. On the other hand, in paper VI only maximally entangled

Bell states are required and thus type II downconversion is sufficient. In both experiments, full state tomography has to be performed for a variety of states. In order to collect enough data for tomography, many photon pairs need to be produced and thus, in order to keep the measurement times reasonably short, a high brightness source for the photon pairs is needed. In the following, ultrabright sources for entangled photons both from type I and type II downconversions are introduced.

After the single photon pairs are created their polarisation state can be locally controlled with phase retarders such as half wave plates or quarter wave plates. The specific state preparations needed in the experiments will be explained in detail later on.

Type I SPDC

In standard type I SPDC two photons with equal polarisation are created [103–105]. The created photons are in a polarisation product state $|\lambda\lambda\rangle$, where λ is orthogonal to the pump beam polarisation. In [106] Kwiat et al. introduced an ultrabright source of polarisation entangled photons based on type I phase matching. The key of the setup is to build a two-crystal geometry, where the optic axes of two identically cut BBO crystals are aligned in perpendicular planes. Now, in this geometry, if the pump is vertically polarised, downconversion will occur only in the first crystal (see Fig. 5.1 (a)) and two photons with horizontal polarisation will be created. If on the other hand, the pump is horizontally polarised, the resulting two photons will instead be vertically polarised (see Fig. 5.1 (b)). Now, linearly polarised (at 45°) pump photon can create a photon in either one of the crystals and the two possible processes are coherent with one another, when the emitted photons are spatially indistinguishable (see Fig. 5.1 (c)). Thus, the created photon pair is in state $\frac{1}{\sqrt{2}}(|HH\rangle + e^{i\phi}|VV\rangle)$. The relative phase ϕ can then be adjusted by controlling the relative phase between the vertical and horizontal components of the original pump, which can be achieved by adding a tiltable quarter wave plate before the crystals.

Another commonly used source for polarisation entangled photon pairs is obtained when in the single crystal geometry type II phase matching conditions are applied [107]. In this case the birefringence effects in the crystal cause the photons to be emitted along two intersecting cones with orthogonal polarisations. When photons are collected only in the intersecting points, they are found in the entangled state $\frac{1}{\sqrt{2}}(|HV\rangle + |VH\rangle)$ (see Fig. 5.2 (a)). However, the brightness of the source is not very high, since the photons can be collected only along two special directions and

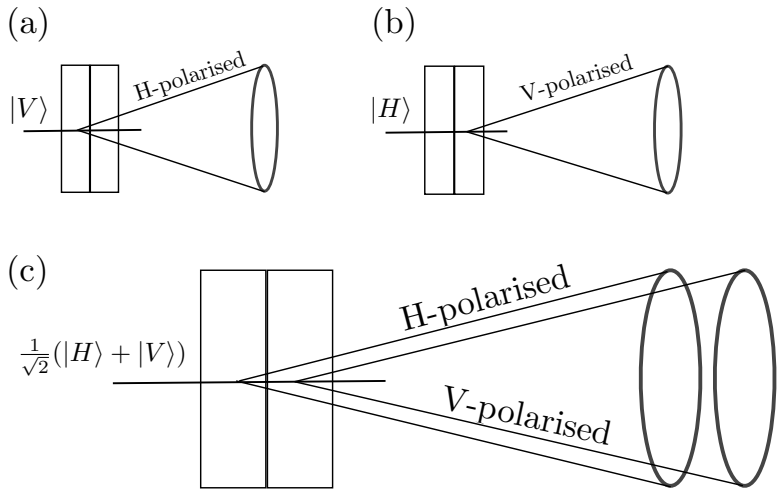

Figure 5.1: Two-crystal geometry for creating polarisation entangled photon pairs with type I phase matching. (a) If the pump is vertically polarised the created pair is in state $|HH\rangle$. (b) If the pump is horizontally polarised the created pair is in state $|VV\rangle$. (c) If the pump photon is 45° polarised, the photon pair is in state $\frac{1}{\sqrt{2}}(|HH\rangle + e^{i\phi}\,|VV\rangle)$.

the other photons will be wasted. In the two-crystal geometry with type I phase matching, instead, all pairs with given frequency are entangled. Also, in this configuration, it is easy to tune the polarisation correlations from factorized to maximally entangled by just controlling the polarisation of the original pump with a half wave plate.

Type II SPDC

As mentioned earlier, the standard SPDC with type II phase matching can be used to produce polarisation entangled photons, but the source lacks in brightness since the highly correlated photons are found only at specific locations and small apertures need to be used for selecting the desired photons. However, recently (see [108] for theoretical proposal and [109] for experimental realisation) a high brightness source using type II phase matching was also developed.

When the original type II source (see Fig. 5.2(a)) with the crossed double ring configuration is used most of the photons emitted from the

crystal are wasted. In order to utilise all the emitted photons a scheme for the production of beamlike downconverted field was developed [110, 111]. In this scheme the original pump pulse is tilted with respect to the optical axis of the crystal in order to change the spatial characteristics of the downconverted field such that the signal and idler photons form two separate beams. Due to the beamlike character now nearly all the emitted photons can be collected and thus the pair detection efficiency is very high.

Now, a two-crystal geometry similar to the one developed for type I SPDC can be put forward for the beamlike type II downconversion (see Fig. 5.2 (b)). Again two BBO crystals with different optic axes are aligned one after another. For original horizontal pump beam polarisation, the first (second) crystal produces beamlike photon pairs in state $|HV\rangle$ ($|VH\rangle$). If now suitable temporal and spatial compensators are used after the downconversion the photons become spatially and temporally indistinguishable and the polarisation state $\frac{1}{\sqrt{2}}(|HV\rangle + |VH\rangle)$ can be created. Now, additional wave guides in the photon paths allow to generate any of the four Bell states.

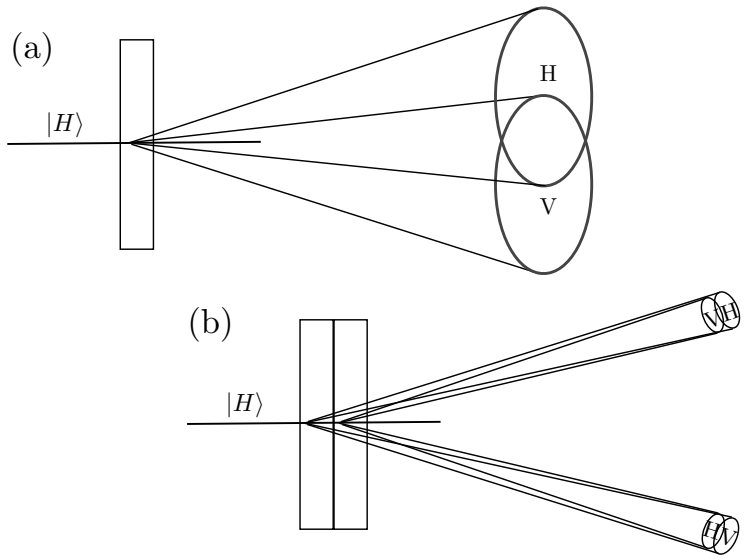

Figure 5.2: Type II SPDC. (a) The standard one crystal geometry with type II phase matching creates a crossed double ring configuration where the entangled photon pairs are collected from the intersection points. (b) Beamlike type II downconversion source for entangled photon pairs with a two-crystal geometry.

Other states besides maximally entangled can not be readily obtained with this scheme, since the relative amplitude between $|HV\rangle$ and $|VH\rangle$ can not be changed by just simply modifying the polarisation of the pump beam. Thus, although being useful for many applications, this scheme for pair production cannot be used when other than maximally entangled states are needed.

5.1.2 Interaction in a quartz plate

A photon, with fixed polarisation and frequency, is described with state $|\lambda\rangle \otimes |\omega\rangle$, where $\lambda = H, V$ gives the polarisation (horizontal or vertical) and ω the frequency of the photon. When the photon travels through a quartz plate of thickness L, the polarisation and frequency are coupled via the unitary operator [112, 113]

$$U(t)\,|\lambda\rangle \otimes |\omega\rangle = e^{in_\lambda \omega t}\,|\lambda\rangle \otimes |\omega\rangle\,, \tag{5.1}$$

where n_λ is the refraction index for a photon with polarisation λ, $t = L/c$ and c is the speed of light. Since the quartz plate is a birefringent media, we have $n_H \neq n_V$. Now, we assume that the photon can be initially prepared in state $|\psi\rangle \otimes |\chi\rangle$, with $|\psi\rangle = \alpha\,|H\rangle + \beta\,|V\rangle$ and $|\chi\rangle = \int d\omega f(\omega)\,|\omega\rangle$. Here, $f(\omega)$ gives the amplitude for the photon to be in a mode with frequency ω, which is normalised as $\int d\omega |f(\omega)|^2 = 1$. Now the unitary dynamics in the quartz plate, given by Eq. (5.1), results in decoherence of superpositions of polarisation state described by the dynamical map

$$\Phi_t : \begin{cases} |H\rangle\langle H| & \mapsto |H\rangle\langle H|, \\ |V\rangle\langle V| & \mapsto |V\rangle\langle V|, \\ |H\rangle\langle V| & \mapsto \kappa^*(t)|H\rangle\langle V|, \\ |V\rangle\langle H| & \mapsto \kappa(t)|V\rangle\langle H|, \end{cases} \tag{5.2}$$

where the decoherence function $\kappa(t) = \int d\omega |f(\omega)|^2 e^{i\omega\Delta n t}$ and $\Delta n = n_V - n_H$.

For two photons, which both go though a quartz plate, i.e. , interact with their local environments via the unitary operator (5.1), the polarisation dynamics can be written as

$$\Phi_t(|ij\rangle\,\langle kl|) = f_{ijkl}(t)\,|ij\rangle\,\langle kl|\,, \tag{5.3}$$

with $i,j,k,l \in \{H,V\}$ $f_{klij} = f^*_{ijkl}$ and

$$f_{ijkl} = \begin{cases} 1 & \text{if} \quad i=k, j=l \\ G(0,t_2) & \text{if} \quad i=k, j=H, l=V \\ G(t_1,0) & \text{if} \quad i=H, k=V, j=l \\ G(t_1,t_2) & \text{if} \quad i=j=H, k=l=V \\ G(t_1,-t_2) & \text{if} \quad i=l=H, j=k=V \end{cases}$$

where

$$G(\tau_1,\tau_2) = \int d\omega_1 \int d\omega_2 P(\omega_1,\omega_2) e^{-i(\omega_1\tau_1+\omega_2\tau_2)}, \tag{5.4}$$

$P(\omega_1,\omega_2)$ is the joint frequency distribution of the two photons and $t_i(t) = \int_0^t \chi_i(t')dt'$. Here, the function $\chi_i(t)$ is 1 for $t_i^{\mathrm{s}} \leq t \leq t_i^{\mathrm{f}}$ and zero otherwise and t_i^{s} and t_i^{f} denote the times the interaction is switched on and switched off in system i. For convenience, we do not explicitly write the time dependence of t_i.

Now, in order to experimentally measure the decoherence dynamics of either one or two photons one has to perform state tomography for the photon(s) for different times. The different points of time can be measured, when the state tomography is performed for alternating quartz plate thicknesses. In the following a method for implementing polarisation state tomography is presented.

5.1.3 Polarisation state tomography

Single qubit tomography can be implemented with a set of four intensity measurements. The first one is performed with a filter, that transmits 50% of the incident light, independent of the polarisation. The second one with a polariser transmitting horizontally polarised light, the third one right-circularly polarised light, and the fourth one light 45° to the horizontal. The subsequent photon counts for the four different configurations allow then to construct the polarisation state via maximum likelihood estimation [114].

It is straightforward to generalise the one qubit scheme for the two qubit case [114]. Now, instead of four intensity measurements, one has to perform sixteen. These sixteen measurements can be performed when polarisers and tunable quarter and half wave plates are mounted in the paths of the two photons. Tuning the angles of the fast axes of the wave plates and performing coincidence detection for each sixteen configurations allows then to reconstruct the polarisation state via maximum likelihood estimation.

5.2 Experimental control of the transition from Markovian to non-Markovian dynamics

For a fixed interaction the characteristics of the open quantum system evolution are determined by the properties of the environment. The environment is usually composed of a large number of degrees of freedom which in general prohibits a systematic engineering of its state. Thus, controlling the evolution of an open system can be very challenging. In paper IV we report an all-optical experiment which allows through careful manipulation of the initial environmental states to drive the open system dynamics from the Markovian to the non-Markovian regime, to control the information flow between the system and the environment, and to determine the degree of non-Markovianity.

The open system dynamics is given by the dynamical map in Eq. (5.2), which describes pure decoherence. Thus the pair of states maximising the non-Markovianity measure (3.5) is known. The pair is $|\psi_{1,2}\rangle = \frac{1}{\sqrt{2}}(|H\rangle \pm |V\rangle)$ and the corresponding trace distance

$$D(\rho_1(t), \rho_2(t)) = |\kappa(t)|. \tag{5.5}$$

Since, the decoherence function is just the Fourier transform of the photon frequency distribution, $\kappa(t) = \int d\omega |f(\omega)|^2 e^{i\omega\Delta n t}$, controlling the frequency spectrum allows us to modify the dynamics of the photon polarisation.

The experimental setup is shown in Fig. 5.3. An ultraviolet Argon-Ion laser is used to pump two 0.3 mm thick BBO crystals cut for type I down conversion process to generate pure two-qubit states. As discussed in section 5.1.1, the polarisation state produced in the downconversion process depends on the initial polarisation of the pump. A fused silica plate (0.04 mm thick and coated with partial reflecting coating on each side, with about 85% reflection probability at 702 nm) is used as a FP cavity. The cavity is mounted on a rotator which can be tilted in the horizontal plane. The tilted cavity can be used for modifying the frequency distribution of the photon. A 4 nm (full width at half maximum) interference filter is further placed after the FP cavity to filter out at most two transmission peaks. The corresponding interference filter in the other arm is 10 nm. The polarisation and frequency degrees of freedom are coupled in a quartz plate in which different evolution times are realised by varying the thickness of the plate. A polarising beam splitter together with a half-wave plate and a

quarter-wave plate is used as a photon state analyser as discussed in section 5.1.3.

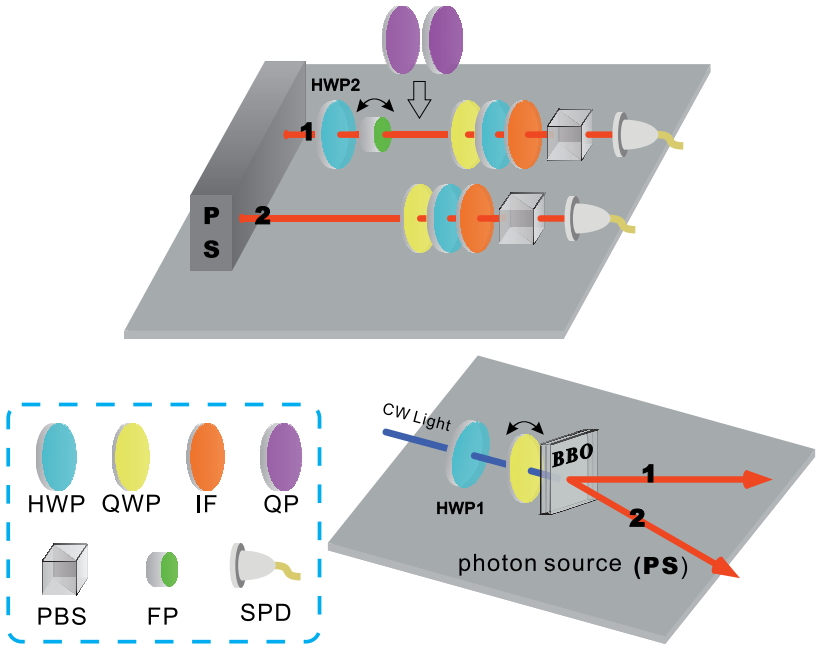

Figure 5.3: The experimental setup for the measurement of the transition from Markovian to non-Markovian dynamics. Here, the abbreviations of the components are: HWP – half wave plate, QWP – quarter wave plate, IF – interference filter, QP – quartz plate, PBS – polarising beamsplitter, FP – Fabry-Perot cavity, and SPD – single photon detector.

In the absence of the FP cavity the frequency distribution can be well approximated by a Gaussian distribution

$$f_G(\omega) = \frac{1}{\sqrt{2\pi\sigma^2}} e^{-\frac{(\omega-\omega_0)^2}{2\sigma^2}}. \tag{5.6}$$

For such distribution the trace distance $D(\rho_1(t), \rho_2(t)) = e^{-\frac{1}{2}\sigma^2(\Delta n t)^2}$ is monotonically decreasing. Thus the information flow is unidirectional and consequently the dynamics is Markovian. Now a FP cavity can be used in order to modify the frequency spectrum and to produce dynamics with a reversed flow of information. In the following we will explain how the tilted cavity influences the spectrum of the photon and thus modifies the open system dynamics.

5.2.1 Environment state control with an FP cavity

Fig. 5.4 shows how tilting the FP cavity modifies the structure of the frequency spectrum and thus the initial environment state $|\chi\rangle = \int d\omega f(\omega) |\omega\rangle$. From the experimental data we can see that the frequency distributions can be well approximated by a sum of two Gaussian functions centred at frequencies ω_k with amplitudes A_k and nearly equal widths σ. Since the tilting angle of the cavity is relatively small the distance between the Gaussian peaks is approximately constant.

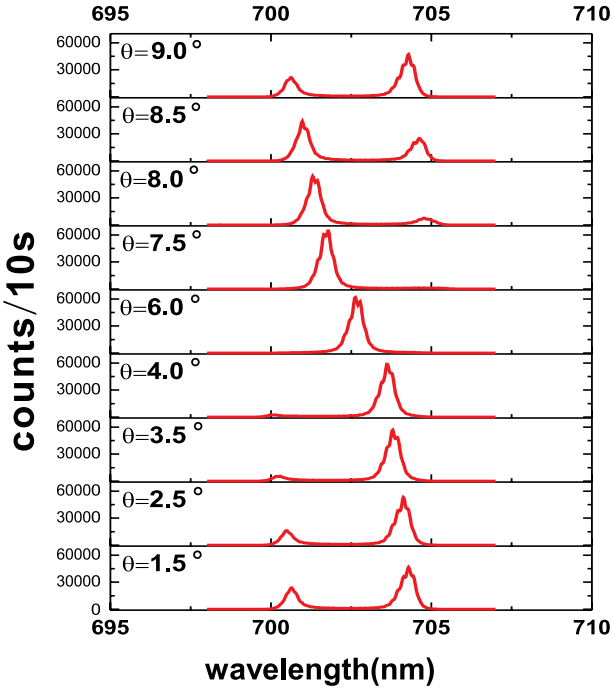

Figure 5.4: The frequency spectrum of the initial state for varying values of the tilting angle θ.

Now, for a double peaked frequency distribution, the decoherence function is

$$|\kappa(t)| = \frac{e^{-\frac{1}{2}\sigma^2(\Delta n t)^2}}{1+A}\sqrt{1+A^2+2A\cos(\Delta\omega\cdot\Delta n t)}, \tag{5.7}$$

where $A_1 = \frac{1}{1+A}$, $A_2 = \frac{A}{1+A}$ and $\Delta\omega = \omega_2 - \omega_1 =$ constant. We see that $|\kappa(t)|$, and therefore also the trace distance $D(\rho_1(t), \rho_2(t))$, oscillates in time for $A \neq 0$ and thus there is information flowing back to the system. In other words, whenever $A \neq 0$ the dynamics is non-Markovian.

5.2.2 Results

The experiment in Fig. 5.3 enables a direct determination of the measure for non-Markovianity. The HWP1 is fixed at zero degree to produce a factorized two-photon state $|HH\rangle$. Photon 2 is directly detected in the SPD at the end of arm 2 as a trigger for state tomography for photon 1. Photon 1 passes through HWP2, preparing it in the state $\frac{1}{\sqrt{2}}(|H\rangle + |V\rangle)$ or $\frac{1}{\sqrt{2}}(|H\rangle - |V\rangle)$. After the subsequent interaction in the quartz plate with the variable length L, a full state tomography is carried out in detector SPD in the end of the arm 1 to determine the polarisation state $\rho_{1,2}(t) = \Phi_t\left(|\varphi_{1,2}\rangle\langle\varphi_{1,2}|\right)$ of photon 1. This allows direct experimental determination of the trace distance $D(\rho_1(t), \rho_2(t))$ between the two possible one-photon states after a certain interaction time t controlled by the length L of the quartz plate. Our experimental results are shown in Fig. 5.5. Increasing the tilting angle of the cavity decreases the relative amplitude A between the peaks in the frequency spectrum and thereby reduces the non-Markovianity of the process until a transition to Markovian dynamics occurs. Further increasing the tilting angle amplifies the relative amplitude again and brings the dynamics back to the non-Markovian regime.

In Ref. [66] an alternative measure for non-Markovianity has been proposed which is based on the idea that a Markovian dynamics leads to a monotonic decrease of the entanglement between the open system and an isomorphic ancilla system, while a non-Markovian dynamics induces a temporary increase of the entanglement. One can show that for the present experiment this measure coincides with (3.5) if one uses the concurrence [115,116] as an entanglement measure. This fact leads to an alternative and independent method for the measurement of the non-Markovianity by means of our experimental setup. Fixing HWP1 to 22.5 degree, we generate a maximally entangled two-photon state. Photon 1 then passes the quartz plate and the composite final state is analysed through two-photon state tomography. Experimental results are shown in Fig. 5.5, clearly demonstrating the equivalence of both measures for non-Markovianity.

5.3 Probing frequency correlations via nonlocal memory effects

In paper VI we demonstrate experimentally that initial correlations between local parts of the environment lead to nonlocal memory effects as predicted theoretically. We further develop a novel design for experimentally ma-

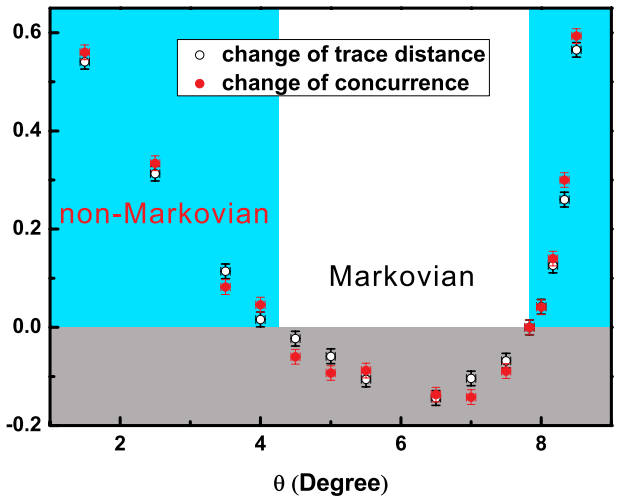

Figure 5.5: The trace distance (a) and the concurrence between the system and the ancilla (b) as a function of the effective path difference for four different values of the tilting angle θ. The solid lines represent the theoretical predictions for $\sigma = 1.8 \times 10^{12}\,\mathrm{Hz}$ and $\Delta\omega = 1.6 \times 10^{13}\,\mathrm{Hz}$. The effective path difference is equal to ΔnL and $\lambda_0 = 702\,\mathrm{nm}$. The experimental error bars due to the counting statistics are smaller than the symbols.

nipulating the correlations of the photonic environments and show that the non-Markovian dynamics of the open system provides a controllable diagnostic tool for the quantification of these correlations.

Let us write a general pure initial polarisation state of a photon pair $|\psi_{12}\rangle = a\,|HH\rangle + b\,|HV\rangle + c\,|VH\rangle + d\,|VV\rangle$. The total initial states are assumed to be product states

$$|\Psi(0)\rangle = |\psi_{12}\rangle \otimes \int d\omega_1 d\omega_2\, g(\omega_1,\omega_2)\,|\omega_1,\omega_2\rangle\,,$$

where $g(\omega_1,\omega_2)$ is the probability amplitude for the photon in arm 1 to have frequency ω_1 and for the photon in arm 2 to have frequency ω_2, with the corresponding joint probability distribution $P(\omega_1,\omega_2) = |g(\omega_1,\omega_2)|^2$. Now, if the photons pass through quartz plates, the dynamics can be described with the map (5.3). The local dynamics for each individual photon $i = 1, 2$ is on the other hand given by Eq. (5.2), with $\kappa_i(t) = \int d\omega P_i(\omega) e^{i\omega\Delta n t_i}$ and $P_i(\omega) = \int d\omega_j P(\omega_i,\omega_j)$, with $j \neq i$.

Now, for a Gaussian joint frequency distribution $P(\omega_1,\omega_2)$ with identical single frequency variance C and correlation coefficient K, the time evolution

of the trace distance corresponding to the Bell-state pair $|\psi_\pm\rangle = \frac{1}{\sqrt{2}}(|HH\rangle \pm |VV\rangle)$ is found to be [117]

$$D(t) = \exp\left[-\frac{1}{2}\Delta n^2 C\left(t_1^2 + t_2^2 - 2|K|t_1 t_2\right)\right]. \tag{5.8}$$

For uncorrelated photon frequencies, i.e. for uncorrelated local environments we have $K = 0$ and the trace distance decreases monotonically, corresponding to Markovian dynamics. However, as soon as the frequencies are anticorrelated, $K < 0$, the trace distance is non-monotonic which signifies quantum memory effects and non-Markovian behavior. On the other hand, the local frequency distributions $P_i(\omega)$ are Gaussian and thus for the single photons the trace distance continuously decreases. Therefore we can conclude, that the system is locally Markovian but globally displays nonlocal memory effects.

In order to demonstrate the appearance of nonlocal memory effects, the experiment presented in Fig. 5.6 was performed. The pair maximising the non-Markovianity measure for the two qubits is $|\psi_\pm\rangle = \frac{1}{\sqrt{2}}(|HH\rangle \pm |VV\rangle)$ [117]. These states are created by using type II spontaneous parametric down conversion. A femtosecond pulse (the duration is about 150 fs and the operation wavelength is at 780 nm, with a repetition rate of about 76 MHz) generated from a Ti:sapphire laser is frequency doubled to pump two 1mm-thick beamlike cut beta barium borate (BBO) crystals creating the two-photon entangled state $\frac{1}{\sqrt{2}}(|HV\rangle \pm |VH\rangle)$. The downconversion photons were collected by single mode fibres in which the entangled state $\frac{1}{\sqrt{2}}(|HV\rangle \pm |VH\rangle)$ is changed to $|\psi_+\rangle$. With the help of QWP1 the entangled state can be easily tuned between $\left|\psi_{12}^+\right\rangle$ (QWP1 is set at 0°) and $\left|\psi_{12}^-\right\rangle$ (QWP1 is set at 90°). Now the size of the anticorrelations (K in Eq. (5.8)) between the photon frequencies can be controlled by tuning the spectrum of the original UV pump pulse.

5.3.1 Control of the initial environment correlations

In the photonic system under study the extent of the nonlocal memory effects is determined by the anticorrelation between the photon frequencies K as can be seen in Eq. (5.8). Since energy is conserved in the down conversion process, decreasing the spectral width δ of the original pump pulse decreases the uncertainty of the sum of the frequencies of the photons, and hence increases the anticorrelation K between the frequencies. We use four different pulse widths in the experiment. The measured frequency

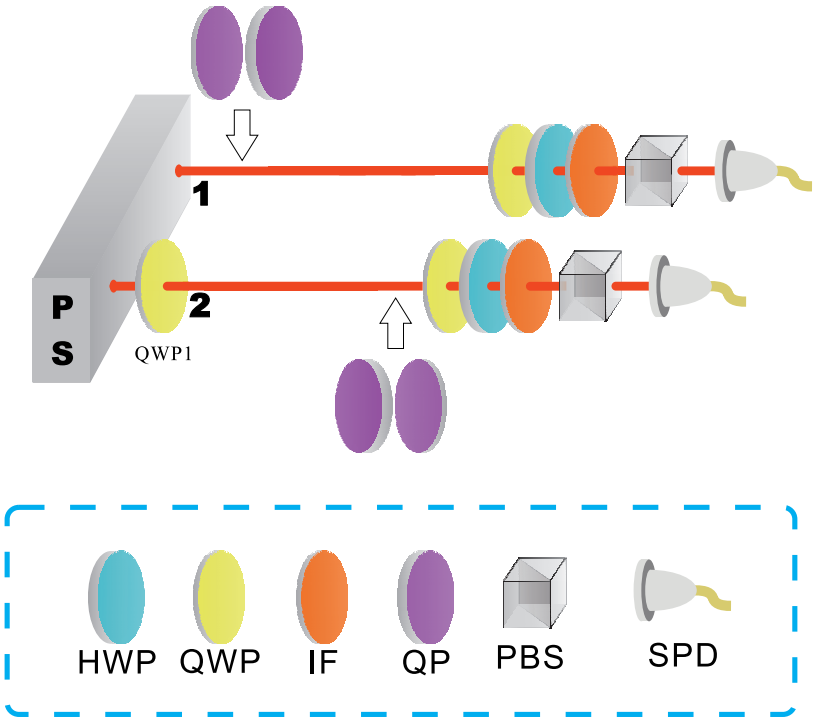

Figure 5.6: Experimental setup for nonlocal memory effects. Maximally entangled photon pairs are generated by parametric down conversion (PDC) with an ultraviolet (UV) pump pulse whose spectral width can be controlled. Then a series of quartz plates are added in arm 1 and arm 2 to realise the local dephasing channels. The final two-photon polarisation state is analysed by state tomography. Key to the components: NC – nonlinear crystal, FP – Fabry-Perot cavity, DM – dispersion medium, HWP – half wave plate, QWP – quarter wave plate, IF – interference filter, QP – quartz plate, PBS – polarising beamsplitter, and SPD – single photon detector.

spectrums of the original pulse are shown in Fig. 5.7. The initial laser source is filtered to 3 nm (FWHM) and then passes through the frequency doubler (1.5 mm thick BiB_3O_4). Hence, the bandwidth of the UV pulse is about 0.52 nm as in Fig. 5.7 (b). In order to obtain a sharper spectrum, as in Fig. 5.7 (a), we insert a thin fused silica plate, which is 0.05 mm thick and coated with a partial reflecting coating on each side, with approximately 75% at 390 nm. For the spectra displayed in Fig. 5.7 (c) and (d), there is no filter before the doubler and no fused silica plate after the doubler, and for Fig. 5.7 (d) the doubler is further displaced by a 0.3 mm-thick BBO.

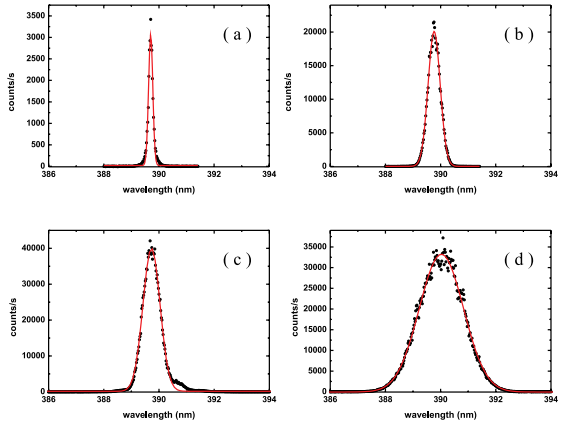

Figure 5.7: The frequency spectra of the ultraviolet pump pulses used for the down conversion process. Full widths at half maximum (FWHM) of the pulse spectra are (a) $\delta = 0.18\,\mathrm{nm}$, (c) $\delta = 0.52\,\mathrm{nm}$, (c) $\delta = 0.73\,\mathrm{nm}$, and (d) $\delta = 1.89\,\mathrm{nm}$. The solid lines represent Gaussian fits of the experimental data.

5.3.2 Results

In the experiment the quartz plates in arm 1 and arm 2 act consecutively, and the magnitude of the initial anticorrelations between the local reservoirs is tuned by changing the spectral width of the pump pulse as in Fig. 5.7. After the photon exits the quartz plates, full two-photon polarisation state tomography is performed and by changing the quartz plate thicknesses, the trace distance dynamics can be worked out. The results for the trace distance dynamics for the different pump pulse widths of Fig. 5.7 are displayed in Fig. 5.8. The panels clearly show how the initial environmental correlations influence the quantum non-Markovianity. First, when only the quartz plate in arm 1 is active, the trace distance decreases monotonically demonstrating that information flows continuously from the system to the environment. When subsequently the quartz plate in arm 1 becomes inactive and the quartz plate in arm 2 active, the trace distance increases highlighting a reversed flow of information from the environment back to the open system.

A further important aspect of the experimental scheme is that it enables to determine the frequency correlation coefficient K of the photon pairs from measurements performed on the polarisation degree of freedom. Thus by performing tomography on a small system we can obtain information

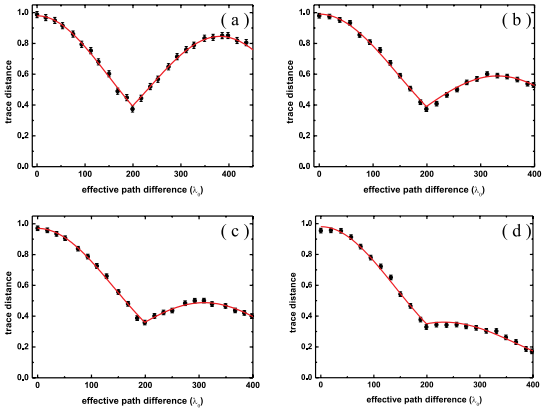

Figure 5.8: Trace distance dynamics for different values of the spectral width of the pump pulse. The widths and the amounts of non-Markovianity are: (a) $\delta = 0.18\,\mathrm{nm}$, $\mathcal{N} = 0.48$, (b) $\delta = 0.52\,\mathrm{nm}$, $\mathcal{N} = 0.23$, (c) $\delta = 0.73\,\mathrm{nm}$, $\mathcal{N} = 0.14$, (d) $\delta = 1.89\,\mathrm{nm}$, $\mathcal{N} = 0.02$. The x-axis represents time measured by the total effective path difference between the horizontal and vertical photons caused by quartz plates in arms 1 and 2 ($\lambda_0 = 780\,\mathrm{nm}$). The y-axis is the trace distance between the time-evolved initial open system states $|\psi_+\rangle$ and $|\psi_+\rangle$. We first add quartz plates in arm 1. When the total effective path difference between horizontal and vertical photons equals $199\lambda_0$, we add quartz plates in arm 2. The solid line shows the fit using the theoretical result of Eq. (5.8). The error bars are due to the counting statistics.

on frequency correlations, difficult to measure directly. Indeed, by fitting the theoretical prediction of Eq. (5.8) to the experimental data, we can obtain a value for K. The fits shown in Fig. 5.8 corresponding to panels (a)-(d) yield the values $K = 0.92$, 0.66, 0.55, and 0.17. Thus we see that the open system (polarisation degrees of freedom) can serve as a quantum probe which allows us to gain nontrivial information on the correlations in the environment (frequency degrees of freedom).

In conclusion, this experiment realised nonlocal quantum dynamical maps of a photonic system and demonstrated experimentally how initial correlations between the local environments of a composite open system induce nonlocal memory effects. While the global dynamics of the open system is non-Markovian, its local subsystems undergo perfectly Markovian dynamics. The measurements performed on the open system dynamics yield also important information about the environment. In fact, we have

seen that a measurement of the non-Markovian evolution of the two-photon polarisation state leads to a novel method for the experimental quantification of frequency correlations. Thus, the open system dynamics can be viewed as a non-Markovian quantum probe which enables to extract non-trivial information on characteristic features of the environment.

Chapter 6

Conclusions

In this Thesis I have discussed various questions underlying the theory of open quantum systems: What is the essence of memory effects in the quantum domain? What is the role of initial system-environment correlations in the open system dynamics? How are memory effects influenced by correlations between local environments? A novel framework in terms of information flow was developed which allowed to give insight into these fundamental questions.

In the first part of the Thesis a theoretical foundation for open quantum systems in terms of information flow was developed. A characterisation of memory effects in the quantum domain was given, which allowed to quantify the degree of non-Markovian behaviour in open system dynamics. This formalism for non-Markovian systems opens the possibility to rigorously study a wide class of open systems which cannot be treated within the standard Markov theory due to, for example, strong system-environment couplings and finite or structured reservoirs. Further, the nonlocal properties of memory effects in bipartite systems were studied and an unexpected feature was revealed: An open system can exhibit memory effects globally even though the local dynamics is Markovian. Moreover, the formulation in terms of information flow allowed to tackle the long standing question on the influence of initial system-environment correlations in the open system dynamics. It was found that the initial correlations manifest themselves as memory effects in the system dynamics and could be thus used to put forward a witness for the initial correlations.

In the second part of the Thesis two all-optical experiments on non-Markovian dynamics were presented. In the first experiment we could through selective preparation of the initial environment states drive the open system from the Markovian to the non-Markovian regime, control the

information flow between the system and the environment, and determine the degree of non-Markovianity. In the second experiment we observed and controlled nonlocal memory effects and provided a novel method to experimentally quantify frequency correlations in photonic environments via polarisation measurements.

Bibliography

[1] R. Agarwal, Phys. Rev. A **2**, 2038 (1970).

[2] R. H. Lehmberg , Phys. Rev. A **2**, 883 (1970).

[3] V. Gorini, A. Kossakowski and E. C. G. Sudarshan, J. Math. Phys. **17**, 821 (1976).

[4] G. Lindblad, Comm. Math. Phys. **48**, 119 (1976).

[5] R. Alicki, and K. Lendi, *Quantum Dynamical Semigroups and Applications* (Springer, Berlin Heidelberg, 2007).

[6] H.-P. Breuer, and F. Petruccione, *The Theory of Open Quantum Systems* (Oxford University Press, Oxford, 2002).

[7] U. Weiss, *Quantum Dissipative Systems 2nd ed.* (World Scientific, Singapore, 1999).

[8] C. W. Gardiner, and P. Zoller, *Quantum Noise* (Springer-Verlag, Berlin, 1999).

[9] P. Haikka, S. McEndoo, G. de Chiara, M. Palma, and S. Maniscalco, Phys. Rev. A **84**, 031602 (2011).

[10] P. Haikka, J. Goold, S. McEndoo, F. Plastina, and S. Maniscalco, Phys. Rev. A **85**, 060101(R) (2012).

[11] T. J. G. Apollaro, C. Di Franco, F. Plastina, and M. Paternostro, Phys. Rev. A **83**, 032103 (2011).

[12] M. Žnidarič, C. Pineda, and I. García-Mata, Phys. Rev. Lett. **107**, 080404 (2011).

[13] I. García-Mata, C. Pineda, and D. Wisniacki, Phys. Rev. A **86**, 022114 (2012).

[14] A. W. Chin, S. F. Huelga, and M. B. Plenio, Phys. Rev. Lett. **109**, 233601 (2012).

[15] R. Vasile et al., Phys. Rev. A **83**, 042321 (2011).

[16] E.-M. Laine, H.-P. Breuer, and J. Piilo, arXiv: quant-ph/1210.8266.

[17] K. H. Hughes, C. D. Christ, and I. Burghardt, J. Chem. Phys. **131**, 024109 (2009).

[18] J. Prior, A. W. Chin, S. F. Huelga, and M. B. Plenio, Phys. Rev. Lett. **105**, 050404 (2010).

[19] P. Siegle, I. Goychuk, P. Talkner, and P. Hänggi, Phys. Rev. E **81**, 011136 (2010).

[20] R. Martinazzo, B. Vacchini, K. H. Hughes, and I. Burghardt, J. Chem. Phys. **134**, 011101 (2011).

[21] B. M. Garraway, Phys. Rev. A **55**, 2290 (1997).

[22] S. Diehl et al., Nature Physics **4**, 878-883 (2008).

[23] H. Krauter et al., Phys. Rev. Lett. **107**, 080503 (2011).

[24] J. Cho, S. Bose, and M. S. Kim, Phys. Rev. Lett. **106**, 020504 (2011).

[25] F. Verstraete, M. M. Wolf, and J. I. Cirac, Nature Physics **5**, 633 (2009).

[26] G. Goldstein et al., Phys. Rev. Lett. **106**, 140502 (2011).

[27] C.J. Myatt et al., Nature **403**, 269 (2000).

[28] H.-P. Breuer and B. Vacchini, Phys. Rev. Lett. **101**, 140402 (2008); Phys. Rev. E **79**, 041147 (2009).

[29] H.-P. Breuer, Phys. Rev. A **70**, 012106 (2004).

[30] J. Rotureau et al., Phys. Rev. Lett. **97**, 110603 (2006).

[31] J. Prior, A. W. Chin, S. F. Huelga, and M. B. Plenio, Phys. Rev. Lett. **105**, 050404 (2010).

[32] J. Piilo, S. Maniscalco, K. Härkönen, and K.-A. Suominen, Phys. Rev. Lett. **100**, 180402 (2008).

[33] J. Piilo, K. Härkönen, S. Maniscalco, and K.-A. Suominen, Phys. Rev. A **79**, 062112 (2009)

[34] H.-P. Breuer, and J. Piilo, EPL **85**, 50004 (2009).

[35] J. T. Stockburger, and H. Grabert, Phys. Rev. Lett. **88**, 170407 (2002).

[36] A. İmamoğlu, Phys. Rev. A **50**, 3650 (1994).

[37] H.-P. Breuer, B. Kappler, and F. Petruccione, Phys. Rev. A **59**, 1633 (1999).

[38] J. Gambetta, T. Askerud, and H. M. Wiseman, Phys. Rev. A **69**, 052104 (2004).

[39] W. T. Strunz, L. Diósi, and N. Gisin, Phys. Rev. Lett. **82**, 1801 (1999).

[40] E. B. Davies, *Quantum Theory of Open Systems* (Academic Press, New York, 1976).

[41] C. Cohen-Tannoudji et al., *Atom-Photon Interactions* (Wiley Science Paperback Series, Hoboken NJ, 1998).

[42] P. Lambropoulos, and D. Petrosyan, *Fundamentals of Quantum Optics and Quantum Information* (Springer, Berlin Heidelberg, 2007).

[43] H. Carmichael, *An open systems approach to quantum optics* (Springer, Berlin Heidelberg, 1993).

[44] S. Hughes, and H. J. Carmichael, Phys. Rev. Lett. **107**, 193601 (2011).

[45] W. Marshall et al., Phys. Rev. Lett. **91**, 130401 (2003).

[46] S. Barnett, and S. Stenholm, Phys. Rev. A **64**, 033808 (2001).

[47] L. Mazzola et al., Phys. Rev. A**81**, 062120 (2010).

[48] S. Daffer et al., Phys. Rev. A **70**, 010304(R) (2004).

[49] A. Shabani, and D. A. Lidar, Phys. Rev. A **71**, 020101(R) (2005).

[50] H.-J. Briegel, and B.-G. Englert, Phys. Rev. A **47**, 3311 (1993).

[51] S. Maniscalco, Phys. Rev. A **75**, 062103 (2007).

[52] S. Nakajima, Progr. Theor. Phys. **20**, 948 (1958).

[53] R. Zwanzig, J. Chem. Phys. **33**, 1338 (1960).

[54] F. Shibata, and N. Hashitsume, Z. Phys. B **34**, 197 (1979).

[55] F. Shibata, Y. Takahashi, and N. Hashitsume, J. Stat. Phys. **17**, 171 (1977).

[56] H.-P. Breuer, J. Gemmer, and M. Michel, Phys. Rev. E **73**, 016139 (2006).

[57] H.-P. Breuer, Phys. Rev. A **75**, 022103 (2007).

[58] E. Andersson, J. D. Cresser, and M. J. W. Hall, J Mod. Opt. **54**, 1695 (2007).

[59] E.-M. Laine, K. Luoma, and J. Piilo, J. Phys. B: At. Mol. Opt. Phys. **45**, 154004 (2012).

[60] D. Chruściński, and A. Kossakowski, Phys. Rev. Lett. **104**, 070406 (2010).

[61] B. Vacchini, and H.-P. Breuer, Phys. Rev. A **81**, 042103 (2010).

[62] N. G. van Kampen, *Stochastic Processes in Physics and Chemistry* (North-Holland Publishing Company, Amsterdam, 1981).

[63] H.-P. Breuer, E.-M. Laine, and J. Piilo, Phys. Rev. Lett. **103**, 210401 (2009).

[64] E.-M. Laine, J. Piilo, and H.-P. Breuer, Phys. Rev. A **81**, 062115 (2010).

[65] M. M. Wolf, J. Eisert, T. S. Cubitt, and J. I. Cirac, Phys.Rev. Lett. **101**, 150402 (2008).

[66] Á. Rivas, S. Huelga, and M. B. Plenio, Phys. Rev. Lett. **105**, 050403 (2010).

[67] R. Vasile, S. Maniscalco, M. G. A. Paris, H.-P. Breuer, and J. Piilo, Phys. Rev. A **84**, 052118 (2011).

[68] S. C. Hou, X. X. Yi, S. X. Yu, and C. H. Oh, Phys. Rev. A **83**, 062115 (2011).

[69] X.-M. Lu, X. Wang, and C. P. Sun, Phys. Rev. A **82**, 042103 (2010).

[70] S. Luo, S. Fu, and H. Song, Phys. Rev. A **86**, 044101 (2012).

[71] D. Chruściński, A. Kossakowski, and Á. Rivas, Phys. Rev. A **83**, 052128 (2011).

[72] M. A. Nielsen, and I. L. Chuang, *Quantum Computation and Quantum Information* (Cambridge University Press, Cambridge, 2000).

[73] G. M. Palma, K.-A. Suominen, and A. K. Ekert, Proc. R. Soc. Lond. A **452**, 567 (1996).

[74] P. Pechukas, Phys. Rev. Lett. **73**, 1060 (1994); Phys. Rev. Lett. **75**, 3021 (1995).

[75] R. Alicki, Phys. Rev. Lett. **75**, 3020 (1995).

[76] G. Lindblad, J. Phys. A **29**, 4197 (1996).

[77] P. Štelmachovič, and V. Bužek, Phys. Rev. A **64**, 062106 (2001); Phys. Rev. A **67**, 029902 (2003).

[78] T. F. Jordan, A. Shaji, and E. C. G. Sudarshan, Phys. Rev. A **70**, 052110 (2004).

[79] H. A. Carteret, D. R. Terno, and K. Życzkowski, Phys. Rev. A **77**, 042113 (2008).

[80] C. A. Rodríguez-Rosario et al., J. Phys. A **41**, 205301 (2008).

[81] A. Shabani, and D. A. Lidar, Phys. Rev. Lett. **102**, 100402 (2009).

[82] A. Brodutch, A. Datta, K. Modi, Á Rivas, and C. A. Rodríguez-Rosario, Phys. Rev. A **87**, 042301 (2013).

[83] C. A. Rodríguez-Rosario, K. Modi, and A. Aspuru-Guzik, Phys. Rev. A **81**, 012313 (2010).

[84] K. Modi, Scientific Reports **2**, 581 (2012).

[85] K. Modi, Open Syst. & Inf. Dyn. **18**, 253 (2011).

[86] C.-F. Li, J.-S. Tang, Y.-L. Li, and G.-C. Guo, Phys. Rev. A **83**, 064102 (2011).

[87] A. Smirne, D. Brivio, S. Cialdi, B. Vacchini, and M. G. A. Paris, Phys. Rev. A **84**, 032112 (2011).

[88] M. Gessner, and H.-P. Breuer, Phys. Rev. Lett. **107**, 180402 (2011).

[89] J. G. Rarity et al., Phys. Rev. Lett. **65**, 1348 (1990).

[90] P. G. Kwiat, A. M. Steinberg, and R. Y. Chiao, Phys. Rev. A **45**, 7729 (1992).

[91] X. Y. Zou, L. J. Wang, and L. Mandel, Phys. Rev. Lett. **67**, 318 (1991).

[92] A. Aspect et al., Phys. Rev. Lett. **47**, 460 (1981).

[93] W. Tittel et al., Phys. Rev. Lett. **81**, 3563 (1998).

[94] G. Weihs, et al., Phys. Rev. Lett. **81**, 5039 (1998).

[95] D. Bouwmeester et al., Nature **390**, 575 (1997).

[96] R. Ursin et al., Nature **430**, 849 (2004).

[97] X.-S. Ma et al., Nature **489**, 269 (2012).

[98] E. Amselem, M. Radmark, M. Bourennane, and A. Cabello, Phys. Rev. Lett. **103**, 160405 (2009).

[99] E. Amselem et al., Phys. Rev. Lett. **108**, 200405 (2012).

[100] J.-S. Tang, C.-F. Li, Y.-L. Li, X.-B. Zou, G.-C. Guo, H.-P. Breuer, E.-M. Laine, and J. Piilo, EPL **97**, 10002 (2012).

[101] S. Cialdi, D. Brivio, E. Tesio, and M. G. A. Paris, Phys.Rev. A **83**, 042308 (2011).

[102] A. Chiuri et al., Scientific Reports **2**, 968 (2012).

[103] P. Hariharan, and B. C. Sanders, Prog. Opt. **36**, 49 (1996).

[104] Z. Y. Ou, and L. Mandel, Phys. Rev. Lett. **61**, 50 (1988).

[105] Y. H. Shih, and C. O. Alley, Phys. Rev. Lett. **61**, 2921 (1988).

[106] P. G. Kwiat, E. Waks, A. G. White, I. Appelbaum, and P. H. Eberhard, Phys. Rev. A **60**, 773 (1999).

[107] P. G. Kwiat et al., Phys. Rev. Lett. **75**, 4337 (1995).

[108] Y.-H. Kim, Phys. Rev. A **68**, 013804 (2003).

[109] X.-L. Niu, Y.-F. Huang, G.-Y. Xiang, G.-C. Guo, and Z.-Y. Ou, Opt. Lett. **33**, 968 (2008).

[110] S. Takeuchi, Opt. Lett. **26**, 843 (2001).

[111] C. Kurtsiefer, M. Oberparleiter, and H. Weinfurter, J. Mod. Opt. **48**, 1997 (2001).

[112] A. J. Berglund, arXiv:quant-ph/0010001v2.

[113] P. G. Kwiat, A. J. Berglund, J. B. Altepeter, and A. G. White, Science **290**, 498 (2000).

[114] D. F. V. James et al., Phys. Rev. A **64**, 052312 (2001).

[115] W. K. Wootters, Phys. Rev. Lett. **80**, 2245 (1998).

[116] P. Rungta et al., Phys. Rev. A **64**, 042315 (2001).

[117] E.-M. Laine, H.-P. Breuer, J. Piilo, C.-F. Li, and G.-C. Guo, Phys. Rev. Lett. **108**, 210402 (2012).